



HAL
open science

A fragment-based approach towards the discovery of N-substituted tropinones as inhibitors of Mycobacterium tuberculosis transcriptional regulator EthR2

Hugues Prevet, Martin Moune, Abdalkarim Tanina, Christian Kemmer, Adrien Herledan, Rosangela Frita, Alexandre Wohlkönig, Marilyne Bourotte, Baptiste Villemagne, Florence Leroux, et al.

► To cite this version:

Hugues Prevet, Martin Moune, Abdalkarim Tanina, Christian Kemmer, Adrien Herledan, et al.. A fragment-based approach towards the discovery of N-substituted tropinones as inhibitors of Mycobacterium tuberculosis transcriptional regulator EthR2. European Journal of Medicinal Chemistry, 2019, 167, pp.426-438. 10.1016/j.ejmech.2019.02.023 . hal-03102744

HAL Id: hal-03102744

<https://hal.science/hal-03102744>

Submitted on 7 Jan 2021

HAL is a multi-disciplinary open access archive for the deposit and dissemination of scientific research documents, whether they are published or not. The documents may come from teaching and research institutions in France or abroad, or from public or private research centers.

L'archive ouverte pluridisciplinaire **HAL**, est destinée au dépôt et à la diffusion de documents scientifiques de niveau recherche, publiés ou non, émanant des établissements d'enseignement et de recherche français ou étrangers, des laboratoires publics ou privés.



Distributed under a Creative Commons Attribution - NonCommercial - NoDerivatives 4.0 International License

A fragment-based approach towards the discovery of N-substituted tropinones as inhibitors of *Mycobacterium tuberculosis* transcriptional regulator EthR2.

Hugues Prevet¹, Martin Moune², Abdalkarim Tanina³, Christian Kemmer⁴, Adrien Herledan¹, Rosangela Frita², Alexandre Wohlkönig⁵, Marilyn Bourotte⁴, Baptiste Villemagne¹, Florence Leroux¹, Marc Gitzinger⁴, Alain R. Baulard², Benoit Déprez¹, René Wintjens³, Nicolas Willand^{*,#1}, Marion Flipo^{#,1}

These authors contributed equally to this work

*nicolas.willand@univ-lille.fr

1. Univ. Lille, Inserm, Institut Pasteur de Lille, U1177 - Drugs and Molecules for living Systems, F-59000 Lille, France
2. Institut Pasteur de Lille, Univ. Lille, CNRS, Inserm, CHU Lille, U1019-UMR8204-CIIL-Centre d'Infection et d'Immunité de Lille, F-59000 Lille, France
3. Unité Microbiologie, Bioorganique et Macromoléculaire (CP206/04), département R3D, Faculté de Pharmacie, Université Libre de Bruxelles, B-1050 Brussels, Belgium
4. Bioversys AG, Hochbergerstrasse 60C, 4057 Basel, Switzerland
5. Structural Biology Brussels, Vlaams Instituut voor Biotechnology (VIB), B-1050 Brussels, Belgium.

Declarations of interest: none

Abstract

Tuberculosis (TB) caused by the pathogen *Mycobacterium tuberculosis*, represents one of the most challenging threat to public health worldwide, and with the increasing resistance to approved TB drugs, it is needed to develop new strategies to address this issue. Ethionamide is one of the most widely used drugs for the treatment of multidrug-resistant TB. It is a prodrug that requires activation by mycobacterial monooxygenases to inhibit the enoyl-ACP reductase InhA, which is involved in mycolic acid biosynthesis. Very recently, we identified that inhibition of a transcriptional repressor, termed EthR2, derepresses a new bioactivation pathway that results in the boosting of ethionamide activation. Herein, we describe the identification of potent EthR2 inhibitors using fragment-based screening and structure-based optimization. A target-based screening of a fragment library using thermal shift assay followed by X-ray crystallography identified 5 hits. Rapid optimization of the tropinone chemical series led to compounds with improved *in vitro* potency.

Keywords

ethionamide, EthR2, fragment-based drug design, tropinone, tuberculosis

Abbreviations

cyHex, cyclohexane; DCE, 1,2-dichloroethane; DCM, dichloromethane; DMAP, 4-dimethylaminopyridine; DMF, dimethylformamide; DMSO, dimethylsulfoxide; DRC, dose-response curve; ETH, ethionamide; EtOH, ethanol; EtOAc, ethyl acetate; HAC, heavy atoms count; MeCN, acetonitrile; MeOH, methanol; Mtb, *Mycobacterium tuberculosis*; PTSA, p-toluenesulfonic acid; SAR,

structure-activity relationships; TB, tuberculosis; tBuOK, potassium tert-butoxide; TEA, triethylamine; TLC, thin layer chromatography; T_m, melting temperature; TSA, thermal shift assay.

1. Introduction

Tuberculosis (TB), a disease caused by *Mycobacterium tuberculosis* (*Mtb*), is the leading cause of death worldwide from a single infectious agent. According to the WHO, 10.0 million people developed tuberculosis in 2017, and 1.3 million HIV-negative people died from TB the same year.[1] Ethionamide (ETH) is a second-line antitubercular drug that is bioactivated by the monooxygenase EthA. EthR, a mycobacterial transcriptional regulator, represses the expression of EthA and thus downregulates ETH bioactivation. A rational design based on the X-ray structure of EthR led to the identification of BDM31343, the first EthR inhibitor able to boost three times ETH activity in mice.[2] The optimization of this compound led to the discovery of BDM41906 that boosts 10 times ETH activity on *Mtb* infected macrophages in the low nanomolar range ($EC_{50} = 60$ nM).[3, 4] BDM41906 also showed boosting activity in a mouse model of *Mtb* infection.[5] In parallel, Tatum et al. described the identification of new series of EthR inhibitors using in silico structure-based screenings.[6]

In recent years, fragment-based approaches have emerged as an alternative approach to high-throughput screening to identify inhibitors of *Mtb* targets.[7, 8] These approaches rely on the screening of small libraries of molecules (~1000 compounds) with low molecular weight (< 300 Da) and high solubility. Usually, although hits identified by this approach display relatively weak biological activities, they are key to reveal compound-target interactions. Fragments can then be optimized using growing, merging or linking strategies to obtain lead compounds with higher affinity for the target. For the past five years, fragment-based approaches have been used successfully to discover and optimize EthR inhibitors.[9-13]

More recently, we have demonstrated that drug resistance to ETH due to mutations in the known bioactivation pathway can be circumvented by derepressing an alternative bioactivation pathway. This can be achieved by the use of a drug-like molecule (SMART-420) that targets a new transcriptional repressor, termed EthR2, allowing ETH bioactivation through this new pathway. This allowed to restore ETH activity on drug-resistant strains but also to increase ETH activity on drug-sensitive strains.[14] The X-ray structure of EthR2, liganded with SMART-420, revealed that the protein belongs to the TetR-type family of repressors. It is an all- α helix protein with a DNA-binding domain at the N-terminal region, showing a Helix-Turn-Helix motif. The C-terminal region presents a dimerization domain and a ligand-binding domain. EthR2 (PDB ID: 5N7O [15]) shares only 14% of sequence identity with EthR (PDB ID: 1U9N), which translates in a rmsd of 3.4 Å over 184 superimposed C α atoms.

In the search for novel chemotypes of EthR2 inhibitors, we initiated a fragment-based approach combining fragment screening, co-crystallization of the hits and chemical modulation of the most potent chemical family. A thermal shift assay was used as a primary assay to identify compounds able to bind to EthR2. Thermal shift assay has been used successfully for several years in drug discovery to identify protein ligands in a high-throughput mode.[16, 17] The principle of this assay is based on monitoring the thermal unfolding of a protein using a hydrophobicity sensitive dye that will undergo a significant increase in quantum yield when bound to the hydrophobic regions of the unfolded protein. Ligands that contribute to the stabilization of a protein in a holo conformation give rise to the increase of the melting temperature of the protein. This variation of T_m (noted ΔT_m) is directly correlated to the affinity of the ligand for the protein. A mammalian assay, previously developed to characterize the mode of action of SMART-420, was further used as a functional secondary assay to measure the potency of the new inhibitors to disrupt the interaction between the transcriptional repressor EthR2 and its DNA operator. This synthetic mammalian gene circuit uses a chimeric

transcription factor, composed of the bacterial transcriptional regulator EthR2 as DNA binding domain that is linked to the virus protein 16 (VP16) activation domain, to monitor transcriptional changes in mammalian cells.[14] Monitoring of the activity of the reporter human placental secreted alkaline phosphatase allows to discriminate if EthR2 can bind to its cognate DNA-operator or if small-molecules may alter or inactivate EthR2 DNA-binding ultimately leading to deactivation of reporter gene expression.

2. Results and discussion

2.1 Screening and X-ray crystallography

An in-house 960-fragment library was screened on the transcriptional regulator EthR2 using a dedicated thermal shift assay (Figure 1). This fluorescence-based assay was initially developed to successfully detect compounds able to bind to EthR and was then adapted to EthR2.[14, 18] Each member of the library was screened at 1 mM and 50 fragments displaying thermal stabilization (ΔT_m) greater than 2 °C were selected for dose-response experiments. Among them, 12 fragments were able to stabilize the transcriptional regulator EthR2 in a dose-dependent manner, giving a hit-rate of 1.25%. These 12 compounds were selected for co-crystallization experiments with EthR2 and the X-ray crystallographic structures of 5 fragment hits (compounds **1-5**, Table 1) bound to EthR2 were obtained.

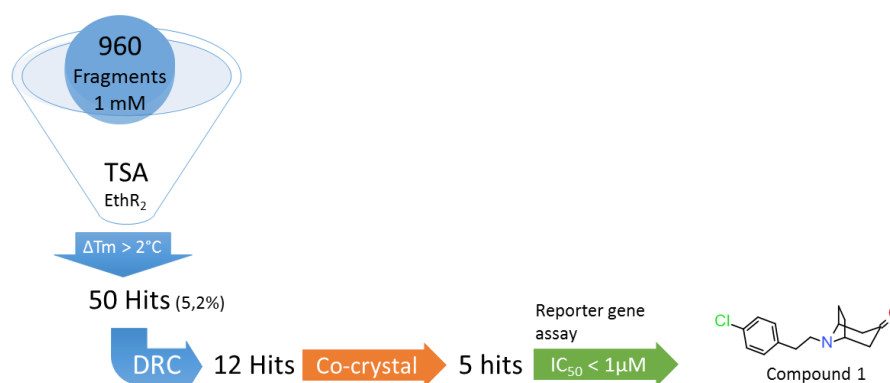


Figure 1. Screening of a 960-fragment library on EthR2 leading to the discovery of the tropinone series.

X-ray diffraction revealed that the 5 molecules bind to the same pocket as SMARt-420. Compound **1** occupies at full occupancy only one of the two monomers of EthR2. The tropinone scaffold is facing the polar area formed by Asp168 and Glu70 with the carbonyl group pointing towards Glu70 and the tertiary amine being H-bonded to Asp168. The bicyclic aliphatic moiety is in contact with Trp100, Ala130 and Ile113. The chlorophenethyl group substituting the nitrogen atom points towards the hydrophobic portal of the ligand binding domain, making close contacts with Leu167 and Met77, and more specifically, a T-shaped π - π stacking occurs between the phenyl ring and Trp100. Compound **2** binds identically the two monomers. The exocyclic nitrogen is H-bonded to Glu70 and the heteroaromatic imidazole ring is engaged in a π -stacking interaction with Trp100. Finally, the isopropyl sulfide substituent occupies the hydrophobic pocket lined by Met74, Met77, Trp100 and Leu167. Compound **3** binds the two monomers in slightly different ways. In both cases the pyridine ring is π -stacked to Trp100 and the urea function is H-bonded to Glu70. However, the propyl substituent binds two different hydrophobic subpockets, one delimited by Leu114, Met172, Trp123 and Phe126, one delimited by Ile113, Phe126 and Val129. Compound **4** also adopts a different binding mode, as two molecules bind only one monomer. The guanidine functions of the two distinct

fragments make ionic interactions with Asp168 and Glu70. Ser134 is H-bonding the closest molecular entity. The two benzothiazole rings are facing the hydrophobic surface area formed by Ile164, Leu167, Trp100, Met77, Met137 and Val73. Finally compound **5** occupies both monomers of EthR2 in the upper part of the ligand binding domain. Indeed, the piperazine ring is H-bonding Asp168 and Ser134, while facing Trp100 and the two methionine residues (Met77 and Met137). The meta-chlorobenzyl group is sandwiched between Leu167 and Leu141.

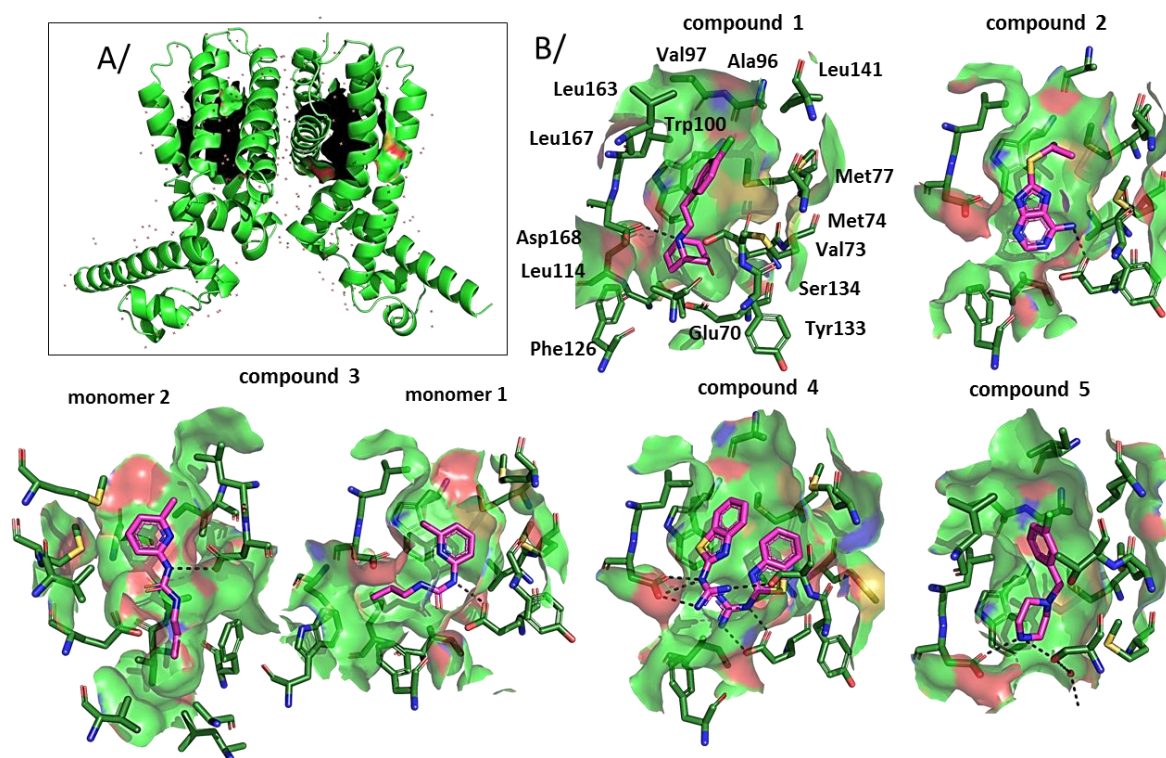


Figure 2: A/ X-ray structure representation of EthR2 as a dimer. The ligand-binding domain is highlighted in black for each monomer. B/ X-ray structure representations of the ligand-binding pocket of EthR2 filled with compound **1** (PDB ID 6HRW), compound **2** (PDB ID 6HRX), compound **3** (PDB ID 6HRY), compound **4** (PDB ID 6HRZ), compound **5** (PDB ID 6HS0). Surface of the ligand binding domain is highlighted. Hydrogen bonds with Asn179 and Asn176 are represented with dotted lines. Colors legend: magenta (compound) or dark green (EthR2) = carbon, dark blue = nitrogen, red = oxygen, yellow = sulfur, light green = chlorine. Images were generated with Pymol.

The ability of these 5 fragments to disrupt the interaction between EthR2 and its DNA-operator was assessed using a EthR2-based reporter gene assay hosted in mammalian cells.[14] In this assay, compounds **3** and **4** were inactive at the highest tested concentration (150 μ M) and compound **1** ($pIC_{50} = 6.0$) was found to be more potent than compounds **2** and **5** ($pIC_{50} = 5.1$ and 5.5 respectively). In addition, compound **1** exhibited the peculiarity of presenting a less flat structure given the presence of the tropinone core, which can improve its physicochemical properties, especially the solubility by avoiding stacking. Therefore, compound **1** was selected for further optimization. To check the selectivity of this compound for EthR2 vs EthR, compound **1** was tested in a mammalian reporter assay using EthR [19] and was totally inactive at the highest concentration tested (30 μ M).

ID structure	cpd	Structure	ΔT_m ($^{\circ}\text{C}$) screening conditions ^a	pIC_{50} ^b
BDM_14272	1		3.4	6.0
BDM_72201	2		2.5	5.1
BDM_72719	3		2.2	< 4
BDM_72170	4		2.8	< 4
BDM_71847	5		3.1	5.5

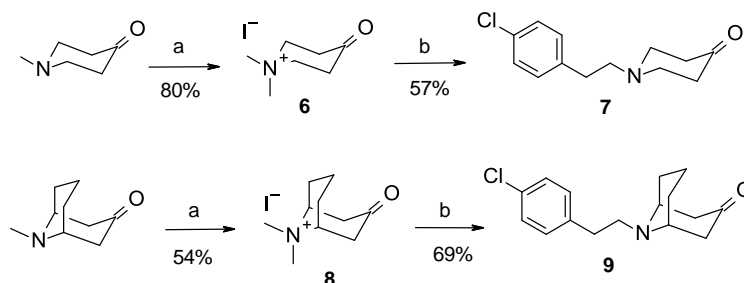
Table 1. Biological activities of compounds 1-5. ^a ΔT_m data were obtained using thermal shift assay with compounds tested at 1 mM. ^b $\text{pIC}_{50} = -\log(\text{IC}_{50})$; IC_{50} represents the concentration of compound that allows the inhibition of 50% of the interaction between EthR_2 and its promoter using a reporter gene assay in mammalian cells.

2.2 Chemistry

A direct synthetic route to obtain *N*-substituted troponone derivatives was developed previously in our lab and we adapted this synthesis to explore structure-activity relationships (SAR) around compound **1**.^[20]

2.2.1. Modifications of the troponone core

First, the importance of the ethylene bridge on the troponone scaffold was evaluated by either removing it (piperidone analogue **7**) or extending it by homologation with the introduction of a pseudopelletierine ring. Compounds **7** and **9** were synthesized in two steps according to a procedure adapted from the literature.^[20] Commercially available *N*-methyl-4-piperidone or pseudopelletierine were reacted with iodomethane in acetone. The tertiary ammonium iodide intermediates **6** and **8** were then refluxed with 4-chlorophenethylamine in a 1/1 mixture of water and ethanol, using potassium carbonate as base (Scheme 1). These two steps reactions afforded compounds **7** and **9** in good yields.

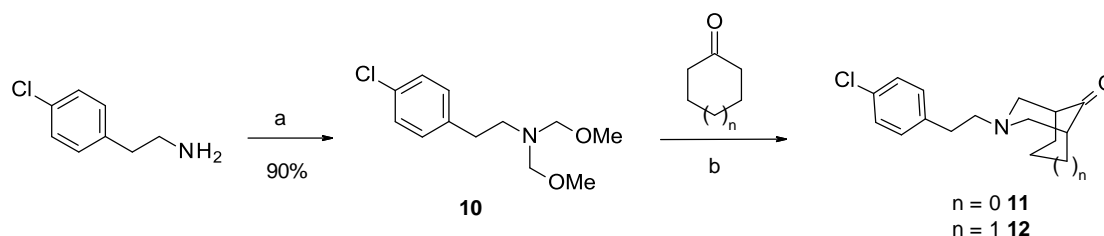


Scheme 1. Synthesis of piperidone and pseudopelletierine derivatives 7 and 9.

Reagents and conditions: (a) CH_3I (1.1 eq), acetone, rt, 1 h, (b) 4- $\text{Cl-C}_6\text{H}_4\text{-(CH}_2\text{)}_2\text{-NH}_2$ (1 eq), K_2CO_3 (2.1 eq), $\text{EtOH/H}_2\text{O}$ (1/1), reflux, 4 h.

We also tested the introduction of the ethylene bridge in α -positions of the carbonyl group. Compound **11** bearing a 3-azabicyclo[3.2.1]octan-8-one ring and compound **12** bearing a 3-

azabicyclo[3.3.1]nonan-9-one were therefore synthesized. These two compounds were obtained in two steps according to Scheme 2. 4-chlorophenethylamine reacted with paraformaldehyde in anhydrous MeOH under basic conditions to give compound **10** that reacted with cyclopentanone or cyclohexanone using methyltrichlorosilane as activator to yield to compounds **11** and **12** respectively [21, 22].

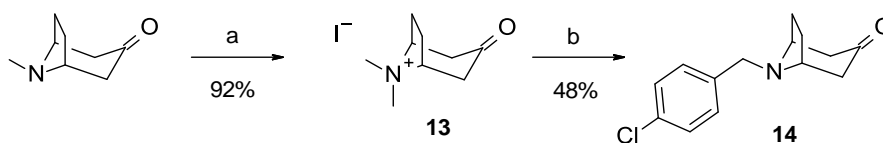


Scheme 2. Synthesis of analogues 11 and 12.

Reagents and conditions: (a) HCHO (3.25 eq), K₂CO₃ (1 eq), anhydrous MeOH, rt, 48 h, (b) CH₃SiCl₃ (2 eq), anhydrous MeCN, rt, 3-8 h.

2.2.2. Modifications of the ethylene linker

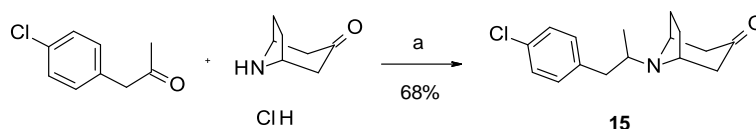
To evaluate the importance of the chain length between the nitrogen atom and the phenyl ring, the phenethyl group was replaced by a benzyl group. Compound **14** was synthesized in two steps as described previously from commercially available tropinone (Scheme 3). 8,8-dimethyl-3-oxo-8-azonia-bicyclo[3.2.1]octane iodide (IDABO, compound **13**) was prepared by reacting iodomethane with tropinone in acetone. IDABO was then refluxed with 4-chlorobenzylamine under basic conditions to give the corresponding *N*-alkylated nortropinone derivative **14**.



Scheme 3. Synthesis of analogue 14.

Reagents and conditions: (a) CH₃I (1.1 eq), acetone, rt, 1 h, (b) 4-Cl-C₆H₄-CH₂-NH₂ (1 eq), K₂CO₃ (2.1 eq), EtOH/H₂O (1/1), reflux, 4 h.

The introduction of a methyl (compound **15**) to evaluate the impact of the steric hindrance in position alpha of the tertiary amine on the activity was carried out by reacting 1-(4-chlorophenyl)propan-2-one with nortropinone hydrochloride under reducing conditions (Scheme 4) [23].

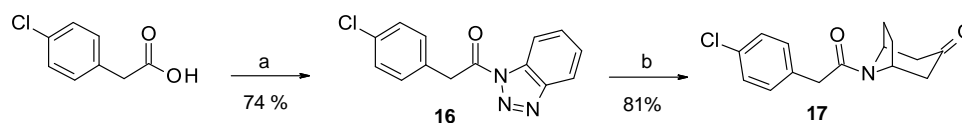


Scheme 4. Synthesis of analogue 15.

Reagents and conditions: (a) TEA (1.1 eq), NaBH(OAc)₃ (1.4 eq), AcOH (1 eq), molecular sieves, DCE, rt, 4 h.

An amide function was introduced to evaluate the importance of the basic nitrogen for the activity. Compound **17** was synthesized in two steps by activating 4-chlorophenylacetic acid using thionyl

chloride and benzotriazole. Compound **16** was then coupled with nortropinone under microwave irradiation (Scheme 5).

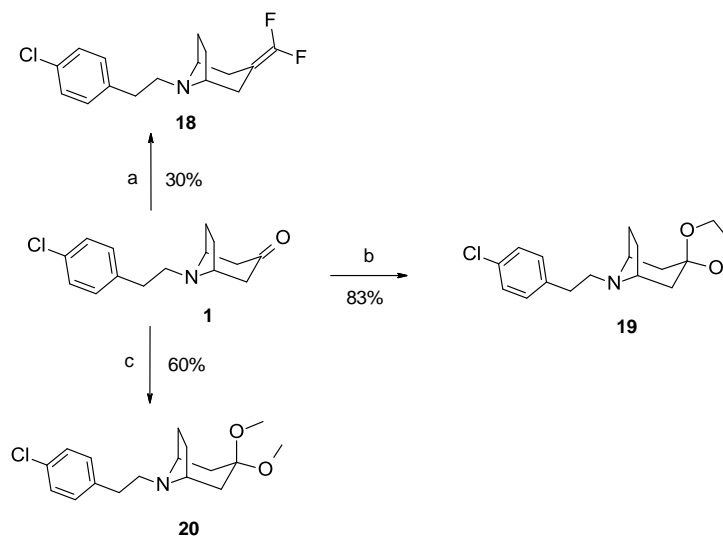


Scheme 5. Synthesis of analogue 17.

Reagents and conditions: (a) SOCl₂ (1 eq), benzotriazole (3 eq), DCM, rt, 24 h, (b) Nortropinone hydrochloride (1.1 eq), DMAP (1.1 eq), CH₂Cl₂, μ W 100 °C, 15 min.

2.2.3. Replacement of the ketone function

The ketone function was replaced by bioisosteres as gem-difluoroolefine, cyclic and acyclic acetals. Compounds **18-20** were synthesized in one step from compound **1**. Compound **18** was obtained by reaction of compound **1** with 2-difluoromethylsulfonylpyridine using potassium tert-butoxide as base [24]. The cyclic acetal **19** was synthesized under microwave irradiation using ethane-1,2-diol and trimethylsilyl chloride in MeCN [25]. The reaction of compound **1** with trimethylorthoformate and *p*-toluenesulfonic acid in MeOH led to acyclic acetal **20**.

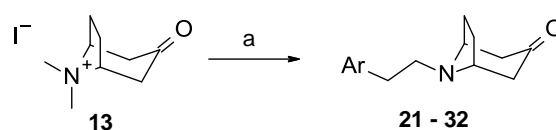


Scheme 6. Synthesis of tropinone derivatives 18-20.

Reagents and conditions: (a) i. t-BuOK (2.2 eq), 2-difluoromethylsulfonylpyridine (1 eq), DMF anhydrous, -25 °C, 96 h, ii. HCl 3M, (b) ethanediol (2.2 eq), Me₃SiCl (4.4 eq), MeCN anhydrous, μ W 80 °C, 25 min, (c) PTSA (2 eq), trimethylorthoformate (5 eq), MeOH anhydrous, μ W 80 °C, 25 min.

2.2.4. Modifications of the 4-chlorophenyl group

In a last step, we investigated the replacement of the 4-chlorophenyl group. Compounds **21-32** were obtained by refluxing IDABO (compound **13**) with substituted phenethylamines under basic conditions to give the corresponding *N*-alkylated nortropinone derivatives (Scheme 7).[20]



Scheme 7. Synthesis of *N*-alkylated nortropinones 21-32.

Reagents and conditions: (a) Ar-(CH₂)₂-NH₂ (1 eq), K₂CO₃ (2.1 eq), EtOH/H₂O (1/1), reflux, 4 h.

2.3 Biological results

In this study, we explored the SAR by modifying the tropinone core (compounds **7**, **9**, **11**, **12**), the ethylene linker (**14**, **15**, **17**), the ketone function (compounds **18-20**) or the 4-chlorophenyl group (compounds **21-32**). All compounds were tested by TSA to evaluate their affinity for the mycobacterial transcriptional regulator EthR2. To avoid possible problems of solubility during the biological evaluation of analogues, compounds were tested at a lower concentration (20 μM) than previously, using the protocol described for the evaluation of the SMART-420 series.[14] For most compounds displaying an affinity for EthR2 ($\Delta T_m > 0.1$ $^{\circ}\text{C}$) we measured their potency to inhibit EthR2/DNA interaction using the EthR2-based reporter gene assay hosted in mammalian cells.

2.3.1. Modifications of the tropinone core

First, we investigated the modification of the tropinone core by removing the ethylene bridge, by extending it by homologation or by moving it in α -positions of the carbonyl group (Table 2). The replacement of the tropinone core (compound **1**) by a piperidone ring (compound **7**) resulted in a decrease in affinity for the protein EthR2 ($\Delta T_m = 0.3$ $^{\circ}\text{C}$). On the contrary, the affinity and the potency are preserved when the pseudopelletierine core (compound **9**) is introduced. These results suggest that an ethylene or propylene bridge connecting the two carbon atoms in β position of the carbonyl function is necessary to improve the affinity. Moreover, the position of this bridge is important, since a loss of affinity is observed when the bridge is introduced at α positions of the carbonyl function regardless of its size (compound **11**, $\Delta T_m = 0.1$ $^{\circ}\text{C}$ and compound **12**, $\Delta T_m < 0$ $^{\circ}\text{C}$).

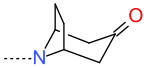
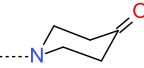
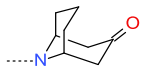
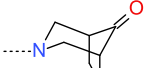
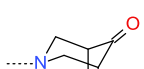
Cpd	R1	ΔT_m ($^{\circ}\text{C}$) SAR conditions ^a	pIC_{50} ^b
1		0.6	6.0
7		0.3	ND
9		0.6	5.8
11		0.1	ND
12		-0.1	ND

Table 2. Biological activities of compounds 1, 7, 9, 11 and 12.
^a compound tested at 20 μM ; ^b $\text{pIC}_{50} = -\log(\text{IC}_{50})$; ND: not determined

2.3.2. Modifications of the ethylene linker

In a second step, the ethylene linker was modified (Table 3). These modifications had a deleterious effect on affinity. Indeed, the reduction of the chain length (compound **14**, $\Delta T_m = 0.0$ $^{\circ}\text{C}$) was not

tolerated and the introduction of a methyl group in α position of the nitrogen atom (compound **15**) led to a compound with a very low affinity for the protein ($\Delta T_m = 0.1$ °C) suggesting that steric hindrance is not tolerated in this position. The introduction of an amide function (compound **17**) was also detrimental to affinity ($\Delta T_m < 0$ °C). This result shows the importance of the basicity of the amine function and can be rationalized by looking at the co-crystallographic structure between **1** and EthR2 (figure 2) in which the nitrogen atom establishes a H-bond with Asp168 side chain.

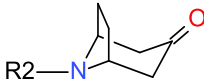
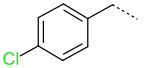
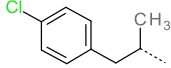
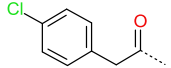
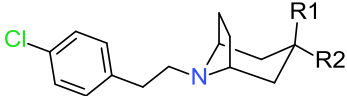
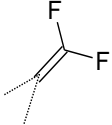
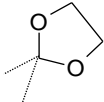
		
Cpd	R2	ΔT_m (°C) SAR conditions ^a
14		0.0
15		0.1
17		-0.1

Table 3. Biological activities of compounds 14, 15, 17.
^a compound tested at 20 μ M

2.3.3. Modifications of the ketone function

The ketone function was replaced by a difluoroethylene function as isoster (compound **18**) [26]. This led to a compound with the same affinity for the protein ($\Delta T_m = 0.6$ °C) but surprisingly inactive in the cellular assay. The replacement of the ketone by acetal groups (compounds **19** and **20**) was not tolerated (Table 4). This result is consistent with the binding mode of compound **1** to EthR2 (Figure 2) where the ketone is facing Glu70. Therefore, its replacement by acetal functions may impair the binding due to steric hindrance.

			
Cpd	R1, R2	ΔT_m (°C) SAR conditions ^a	pIC_{50} ^b
1		0.6	6.0
18		0.6	< 4.8
19		0.1	< 4.8

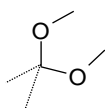
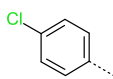
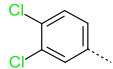
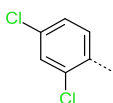
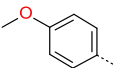
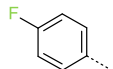
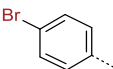
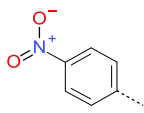
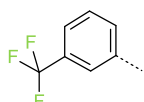
20		0.2	< 4.8
----	---	-----	-------

Table 4. Biological activities of compounds 18-20.
^a compound tested at 20 μ M; ^b $pIC_{50} = -\log(IC_{50})$; ND: not determined

2.3.4. Modifications of the 4-chlorophenyl group

To further explore the SAR, the 4-chlorophenyl group was replaced by aromatic rings substituted in different positions with electron donating or withdrawing groups (Table 5).

Cpd	R3	ΔT_m ($^{\circ}$ C) SAR conditions ^a	pIC_{50} ^b
1		0.6	6.0
21		0.1	5.0
22		1.0	6.0
23		0.2	5.7
24		0.0	ND
25		0.6	5.8
26		0.3	ND
27		0.4	5.6
28		1.0	6.1
29		-0.2	ND
30		1.8	6.7
31		-0.1	ND

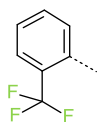
32		0.3	ND
-----------	---	-----	----

Table 5. Biological activities of compound 1 and compounds 21-32.
^a compound tested at 20 μ M; ^b pIC₅₀ = -log(IC₅₀); ND: not determined

Replacing the 4-chlorophenyl group with an unsubstituted phenyl group (compound **21**) led to a much less active compound ($\Delta T_m = 0.1$ °C, pIC₅₀ = 5.0). The introduction of a second chlorine atom at position 3 on the phenyl ring (compound **22**) led to a compound slightly more active than the reference compound **1** ($\Delta T_m = 1.0$ °C, pIC₅₀ = 6.0). In contrast, the introduction of a second chlorine atom at position 2 (compound **23**) decreased the biological activities ($\Delta T_m = 0.2$ °C, pIC₅₀ = 5.7). This result suggests that position 2 of the phenyl ring may be sensitive to steric hindrance. The replacement of the 4-chlorophenyl group by a pyridine (compound **24**) is not tolerated ($\Delta T_m = 0.0$ °C). Substitution of the phenyl ring with an electron-donating group such as methoxy (compound **26**) reduced affinity ($\Delta T_m = 0.3$ °C), whereas introduction of a methyl group (compound **25**) led to a compound as active as reference compound **1** ($\Delta T_m = 0.6$ °C, pIC₅₀ = 5.8). The replacement of the chlorine atom by a smaller fluorine atom (compound **27**) led to a less active compound ($\Delta T_m = 0.4$ °C, pIC₅₀ = 5.6) while the introduction of a larger bromine atom (compound **28**) increased the activity ($\Delta T_m = 1.0$ °C, pIC₅₀ = 6.1) showing that a bulky atom is tolerated in this position. The introduction of a trifluoromethyl group in position 4 of the phenyl ring (compound **30**) led to a compound having a better affinity for EthR2 as well as a better potency than the compound **1** ($\Delta T_m = 1.8$ °C, pIC₅₀ = 6.7). This result suggests that steric hindrance or hydrophobicity at the para position of the phenyl ring are important criteria for activity. Substitution of the phenyl ring in para position with a nitro group (compound **29**) strongly affected affinity ($\Delta T_m < 0$ °C), which suggests that an electron withdrawing group on the aromatic ring is not the only parameter necessary for the affinity of the compounds. Substitutions of the phenyl ring in ortho and meta positions with a trifluoromethyl group (compounds **32** and **31**) strongly reduced affinity ($\Delta T_m = 0.3$ °C and $\Delta T_m < 0$ °C respectively), confirming the steric hindrance issue aforementioned with compound **23**.

For compounds evaluated in both biological assays, we plotted the potency (pIC₅₀) as a function of the affinity (ΔT_m). Interestingly, we observed a strong correlation ($R^2 = 0.87$) between pIC₅₀ and ΔT_m (Figure 3) ascertaining that the potency of the compounds to disrupt the interaction between EthR2 and DNA is linked to their binding to EthR2.

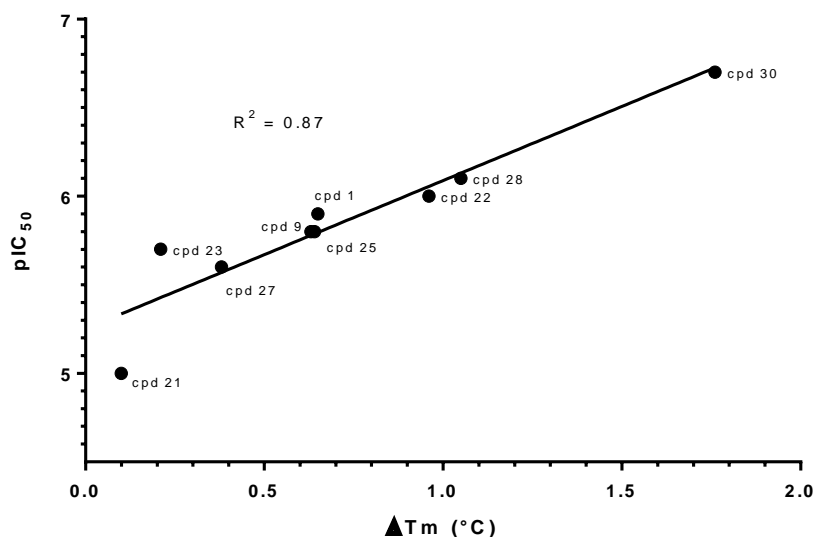


Figure 2. pIC₅₀ versus ΔTm

In order to measure the capacity of the compounds to boost ten times the activity of ETH, nine compounds (**1**, **9**, **21**, **22**, **24**, **25**, **27**, **28**, **30**) were tested on *M. tuberculosis* with subactive doses of ETH (MIC/10 = 0.1 μg/mL). Unfortunately, none of the compounds was able to boost ETH bioactivation at concentrations up to 30 μM through the EthR2/EthA2 pathway. This may be due to a lack of bacterial membrane permeability.

2.4. Co-crystallization

Compounds **9** and **30** were successfully co-crystallized with the repressor EthR2 (Refinement statistics listed in Table 6). The two molecules have similar binding mode that is also similar to the one of compound **1**. Both molecules are found at full occupancy only in one of the two monomers of EthR2, and their tertiary amines are H-bonded to Asp168 side chain. Similarly to compound **1**, the aromatic ring is in contact with Ser134, Ile164, Leu167, Met177, Trp100 and Thr138 and the bicyclic moiety is in contact with Ala130, Ile113, Phe126, Trp100, Met74 and Val73.

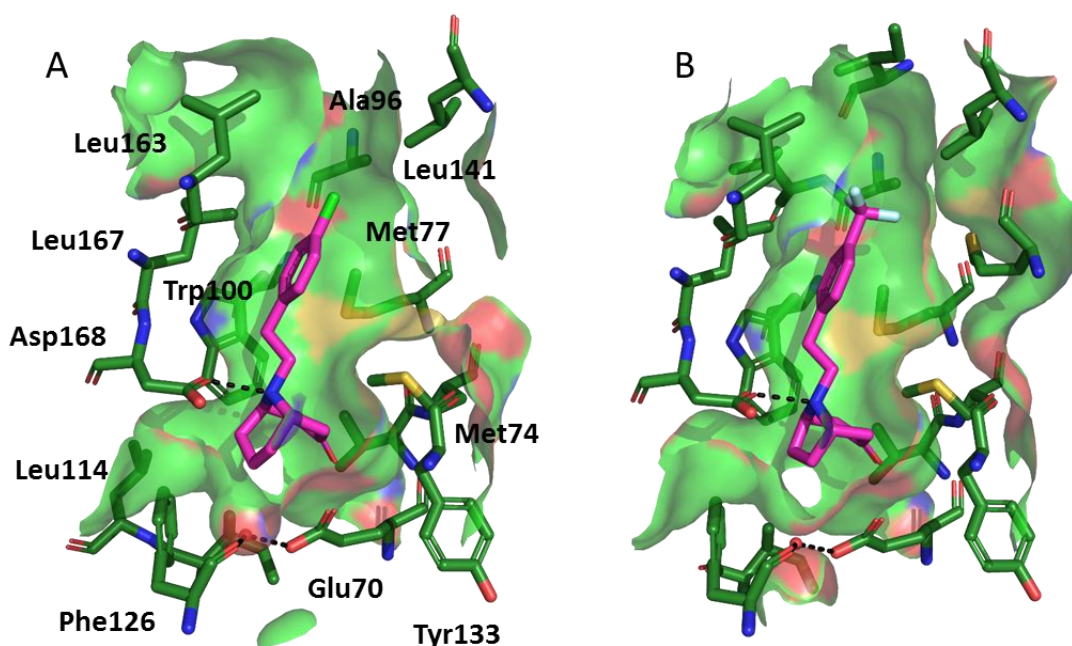


Figure 4: (A) X-ray structure representations of the ligand-binding pocket of EthR2 filled with compound **9** (PDB ID 6HS1). (B) X-ray structure representations of the ligand-binding pocket of EthR2 filled with compound **30** (PDB ID 6HS2). Surface of the ligand binding domain is highlighted. Hydrogen bonds with Asn179 and Asn176 are represented with dotted lines. Colors legend: magenta (compound) or dark green (EthR2) = carbon, dark blue = nitrogen, red = oxygen, yellow = sulfur, light green = chlorine, light blue = fluorine. Images were generated with Pymol.

3. Conclusion

Through a fragment-based approach, we first identified five new chemical series as ligands of the mycobacterial transcriptional regulator EthR2. By combining structure-based design from the protein–ligand complexes obtained by co-crystallization, with *in vitro* assays (target-based and functional), we were able to study structure-activity relationships and delineate the key molecular features that are essential for the molecular recognition of the analogues in the tropinone series by EthR2. Compounds **9**, **22** and **28** were equipotent as the hit, and the trifluoromethyl derivative (compound **30**) was more potent at disrupting the interaction between the transcriptional repressor and its targeted promoter ($pIC_{50} = 6.7$). Interestingly, this compound displayed a high ligand efficiency index ($LE = 0.44 = (1.37 * pIC_{50}) / (HAC)$; HAC: Heavy Atoms Count). Optimization of the physico-chemical properties in this series will be pursued in order to find compounds capable of boosting ethionamide activity in *M. tuberculosis* infected macrophages.

Acknowledgements

We thank H el ene Cristini, Guillaume Blanc and Birgit Schellhorn for technical assistance. This work was supported by l'Agence Nationale de la Recherche (ANR), France (Tea-4-Two, ANR-14-CE14-0027-01), PRIM (NewBio4Tb), Institut National de la Sant e et de la Recherche M edicale, Universit e de Lille, Institut Pasteur de Lille, Centre National de la Recherche Scientifique, R egion Hauts-de-France (convention no.12000080), and Soci et e d'Acc el eration du Transfert de Technologie Nord. The NMR facilities were funded by the R egion Nord-Pas de Calais (France), the Minist ere de la Jeunesse, de l'Education Nationale et de la Recherche (MJENR), the Fonds Europ eens de D eveloppement R egional (FEDER) and Lille University. Ren e Wintjens is a Research Associate at the Belgian National Fund for Scientific Research (FRS-FNRS). We are indebted to the ID30A-1 (MASSIF-1) ESRF (proposals MX1866

and MX1960) and to the SOLEIL-PROXIMA-I/II (BAG proposal 20171555) synchrotron facilities for beam-time allocations.

4. Experimental section

4.1. Chemistry

Solvents for synthesis, analysis and purification were purchased as analytical grade from commercial suppliers and used directly without further purification. Chemical reagents were purchased from Acros, Aldrich, Fluka, Merck, Maybridge, Fluorochem, TCI or Alfa Aesar as reagent grade and used without further purification.

HPLC-MS analysis was performed on two different HPLC-MS systems:

LC-MS Waters Alliance Micromass ZQ 2000 system was equipped with a Waters 2747 sample manager, a Waters 2695 separations module, a Waters 2996 photodiode array detector (200-800 nm) and a Waters Micromass ZQ2000 detector (scan 100-800).

LC-MS Waters 3100 Mass Detectors system was equipped with a Waters 2767 sample manager, a Waters 515 HPLC pump, a Waters Systems Fluidics Organizer, a Waters 2545 Binary Gradient Module, a Waters 2487 Dual λ Absorbance (215 nm and 254 nm) detector and a Waters 3100 Mass detectors.

XBridge C18 column (3.5 μ m particle size, dimensions 50 mm x 4.6 mm) was used for HPLC analysis. The injection volume was 20 μ L. A mixture of water and acetonitrile was used as mobile phase in gradient-elution. The pH of the mobile phase was adjusted with HCOOH and NH₄OH to form a buffer solution at pH 3.8 or pH 9.2. The analysis time was 5 minutes (at a flow rate at 2 mL/min), 10 minutes (at a flow rate at 1 mL/min) or 30 minutes (at a flow rate at 1 mL/min). Purity (%) was determined by reversed phase HPLC, using UV detection (215 nm), and all isolated compounds showed purity greater than 95%.

HRMS analysis was performed on a LCT Premier XE Micromass, using a C18 X-Bridge 3.5 μ m particle size column, dimensions 50 mm * 4.6 mm. A gradient starting from 98% H₂O 5 mM Ammonium Formate pH=3.8 and reaching 100% CH₃CN 5 mM Ammonium Formate pH=3.8 within 3 min at a flow rate of 1 mL/min was used.

NMR spectra were recorded on a Bruker DRX-300 spectrometer. The results were calibrated to signals from the solvent as an internal reference [e.g. 5.32 (residual CD₂Cl₂) and 53.84 (CD₂Cl₂) ppm, 2.50 (residual DMSO-d₆) and 39.52 (DMSO-d₆) ppm for ¹H and ¹³C NMR spectra, respectively]. Chemical shifts (δ) are in parts per million (ppm) downfield from tetramethylsilane (TMS). The assignments were made using one-dimensional (1D) ¹H and ¹³C spectra and two-dimensional (2D) HSQC-DEPT, COSY and HMBC spectra. NMR coupling constants (J) are reported in Hertz (Hz), and splitting patterns are indicated as follows: s for singlet, brs for broad singlet, d for doublet, t for triplet, a for quartet, quin for quintet, sex for sextet, dd for doublet of doublet, ddd for doublet of doublet of doublet, dt for doublet of triplet, qd for quartet of doublet, m for multiplet, δ for chemical shift, J for coupling constant.

Flash chromatography was performed using silica gel cartridges. The reactions were monitored by thin layer chromatography on silica gel pre-coated F254 Merck plates and the resulting eluted plates were viewed under ultraviolet light at 254 nm and/or stained using a solution potassium permanganate.

General procedure A for the synthesis of the tertiary ammonium iodide salt.

The corresponding cyclic ketone (1 eq.) was dissolved in acetone (C = 1 M) under stirring. Methyl iodide (1.1 eq.) was added dropwise. Reaction mixture was stirred at RT for 1 hour. Precipitate was filtered and washed with acetone and with cyclohexane/ethyl acetate solution (1/1). The resulting solid was dried under reduced pressure to give the desired compound.

1,1-Dimethylpiperidin-1-ium-4-one iodide (**6**).

The title compound was synthesized according the general procedure **A** using the *N*-methyl-4-piperidone as starting material. Yield: 80% as a white solid. ¹H-NMR (DMSO-d₆): δ (ppm) 3.74 (t, *J* = 7.1 Hz, 2H), 3.36 – 3.33 (m, 1H), 3.32 (s, 3H), 3.26 (s, 3H), 2.72 – 2.68 (m, 2H), 1.89 – 1.84 (m, 3H).

9,9-Dimethyl-9-azoniabicyclo[3.3.1]nonan-3-one iodide (**8**)

The title compound was synthesized according the general procedure **A** using the pseudopelletierine as starting material. Yield: 54% as a white solid. ¹H-NMR (DMSO-d₆): δ (ppm) 3.93 - 3.89 (m, 2H), 3.36 (s, 3H), 3.32 (s, 3H), 3.26 - 3.24 (m, 1H), 2.60 - 2.54 (m, 2H), 2.42 - 2.28 (m, 2H), 1.80 - 1.74 (m, 2H), 1.64 - 1.56 (m, 1H), 1.39 - 1.22 (m, 2H).

8,8-Dimethyl-8-azoniabicyclo[3.2.1]octan-3-one iodide (**13**)

The title compound was synthesized according the general procedure **A** using the tropinone as starting material. Yield: 92% as a white solid. ¹H-NMR (DMSO-d₆): δ (ppm) 4.17 (m, 2H), 3.39 (s, 3H), 3.19 (s, 3H), 2.97 (m, 2H), 2.65 (m, 2H), 2.50 (m, 2H), 1.95 (m, 2H).

General procedure B for the alkylation of the tertiary ammonium iodide salt.

To a solution of the appropriate amine (1 eq.) in EtOH (C = 0.5 M) was added a solution of K₂CO₃ (2.1 eq.) in water (C = 3 M). The resulting solution was refluxed and a solution of the appropriate tertiary ammonium iodide (1.1 eq.) in water (C = 0.8 M) was added dropwise. The reaction mixture was refluxed for 4 hours. The reaction was monitored by TLC. After completion, the reaction was cooled down to RT and volatiles were removed under vacuum. The residue was extracted with DCM (3x), washed with brine (1x), dried over MgSO₄ and reduced *in vacuo*. The residue was purified by flash chromatography to give the desired product.

8-[2-(4-Chlorophenyl)ethyl]-8-azabicyclo[3.2.1]octan-3-one (**1**)

The title compound was synthesized according the general procedure **B** using the 8,8-dimethyl-8-azoniabicyclo[3.2.1]octan-3-one iodide (**13**) and 2-(4-chlorophenyl)ethylamine as starting materials. Yield: 76%. ¹H-NMR (CD₂Cl₂): δ (ppm) 7.30 (d, *J* = 8.7 Hz, 2H), 7.23 (d, *J* = 8.5 Hz, 2H), 3.58 - 3.53 (m, 2H), 2.88 - 2.79 (m, 4H), 2.63 (dd, *J* = 16.0 Hz, *J* = 4.5 Hz, 2H), 2.15 (d, *J* = 15.8 Hz, 2H), 2.05 - 2.00 (m, 2H), 1.59 (d, *J* = 7.8 Hz, 2H). ¹³C-NMR (CD₂Cl₂): δ (ppm) 209.4, 139.2, 131.6, 130.2, 128.3, 58.9, 52.1, 47.5, 35.2, 27.8. HRMS (TOF, ES+) *m/z* [M+H]⁺ calculated for C₁₅H₁₉NOCl 264.1155, found 264.1159.

1-[2-(4-Chlorophenyl)ethyl]piperidin-4-one (**7**)

The title compound was synthesized according the general procedure **B** using the 1,1-dimethylpiperidin-1-ium-4-one iodide (**6**) and 2-(4-chlorophenyl)ethylamine as starting materials. Flash chromatography cyHex to cyHex/EtOAc 7/3. Yield: 57%. ¹H-NMR (CD₂Cl₂): δ (ppm) 7.29 (d, *J* = 8.8 Hz, 2H), 7.21 (d, *J* = 8.6 Hz, 2H), 2.85 - 2.68 (m, 8H), 2.43 (t, *J* = 6.3 Hz, 4H). ¹³C-NMR (CD₂Cl₂): δ (ppm) 208.5, 139.1, 131.6, 130.1, 128.3, 58.7, 53.1, 41.2, 33.2. HRMS (TOF, ES+) *m/z* [M+H]⁺ calculated for C₁₃H₁₇NOCl 238.0999, found 238.0995.

9-[2-(4-Chlorophenyl)ethyl]-9-azabicyclo[3.3.1]nonan-3-one (**9**)

The title compound was synthesized according the general procedure **B** using the 9,9-dimethyl-9-azoniabicyclo[3.3.1]nonan-3-one iodide (**8**) and 2-(4-chlorophenyl)ethylamine as starting materials.

Flash chromatography cyHex to cyHex/EtOAc 8/2. Yield: 69%. ¹H-NMR (CD₂Cl₂): δ (ppm) 7.30 (d, *J* = 8.5 Hz, 2H), 7.22 (d, *J* = 8.5 Hz, 2H), 3.40 - 3.35 (m, 2H), 2.95 - 2.90 (m, 2H), 2.80 - 2.75 (m, 2H), 2.66 (dd, *J* = 16.4 Hz, *J* = 6.4 Hz, 2H), 2.20 (d, *J* = 16.6 Hz, 2H), 1.94 - 1.82 (m, 2H), 1.57 - 1.41 (m, 4H). ¹³C-NMR (CD₂Cl₂): δ (ppm) 210.7, 139.4, 131.5, 130.3, 128.2, 54.5, 54.2, 42.6, 34.7, 29.7, 16.6. HRMS (TOF, ES+) *m/z* [M+H]⁺ calculated for C₁₆H₂₁NOCl 278.1312, found 278.1319.

2-(4-Chlorophenyl)-*N,N*-bis(methoxymethyl)ethanamine (**10**). Anhydrous K₂CO₃ (1 eq.) was added to a mixture of anhydrous MeOH (C = 2 M) and paraformaldehyde (3.25 eq.). Then, 2-(4-chlorophenyl)ethylamine (1 eq.) was added over a period of 30 minutes and the resulting mixture was stirred for 48 hours at RT. The crude reaction was filtered to remove all solids and the filtrate was concentrated under vacuum. The residue was suspended in anhydrous DCM and filtered. The filtrate was evaporated under reduced pressure to afford 2-(4-chlorophenyl)-*N,N*-bis(methoxymethyl)ethanamine (**10**). Yield: 90%. ¹H-NMR (CD₂Cl₂): δ (ppm) 7.27 (d, *J* = 8.6 Hz, 2H), 7.19 (d, *J* = 8.6 Hz, 2H), 4.24 (s, 4H), 3.20 (s, 6H), 3.11 - 3.06 (m, 2H), 2.83 - 2.78 (m, 2H).

Procedure for the synthesis of compounds 11 and 12.

To a mixture of the appropriate cyclic ketone (cyclopentanone or cyclohexanone, 1 eq.) and 2-(4-chlorophenyl)-*N,N*-bis(methoxymethyl)ethanamine (**10**, 2 eq.) in anhydrous MeCN (C = 1 M) was added trichloromethylsilane (2 eq.). The mixture was stirred at RT for 3 to 8 hours (monitoring done by TLC, 2,4-DNPH staining), quenched with an aqueous saturated NaHCO₃ and extracted with EtOAc (3x). The combined organic layers were washed with brine (1x), dried over MgSO₄ and concentrated under vacuum. The residue was purified by flash chromatography to give the desired final product (**11** and **12**).

3-[2-(4-Chlorophenyl)ethyl]-3-azabicyclo[3.2.1]octan-8-one (**11**)

Flash chromatography cyHex to cyHex/DCM/EtOAc 8/1/1. Yield: 40%. ¹H-NMR (CD₂Cl₂): δ (ppm) 7.29 (d, *J* = 8.4 Hz, 2H), 7.22 (d, *J* = 8.8 Hz, 2H), 3.06 - 3.01 (m, 2H), 2.81 - 2.75 (m, 2H), 2.72 - 2.67 (m, 2H), 2.56 (d, *J* = 10.4 Hz, 2H), 2.15 - 2.10 (m, 2H), 1.92 - 1.86 (m, 2H), 1.84 - 1.78 (m, 2H). ¹³C-NMR (CD₂Cl₂): δ (ppm) 220.0, 139.7, 132.0, 130.1, 128.2, 61.8, 56.7, 45.4, 33.1, 22.6. HRMS (TOF, ES+) *m/z* [M+H₂O+H]⁺ calculated for C₁₅H₂₁NO₂Cl 282.1261, found 282.1252.

3-[2-(4-Chlorophenyl)ethyl]-3-azabicyclo[3.2.1]octan-8-one (**12**)

Flash chromatography petroleum ether to petroleum ether/(DCM-EtOH 3/1) 9/1. Yield: 25%. ¹H-NMR (CD₂Cl₂): δ (ppm) 7.30 (d, *J* = 8.6 Hz, 2H), 7.21 (d, *J* = 8.6 Hz, 2H), 3.23 (dd, *J* = 12.6 Hz, *J* = 1.6 Hz, 2H), 2.81 (t, *J* = 7.7 Hz, 2H), 2.65 - 2.51 (m, 5H), 2.33 - 2.29 (m, 2H), 2.14 - 2.06 (m, 2H), 2.04 - 1.91 (m, 2H), 1.41 - 1.33 (m, 1H). ¹³C-NMR (CD₂Cl₂): δ (ppm) 217.9, 139.6, 131.9, 130.1, 128.2, 60.3, 58.4, 48.0, 34.8, 33.1, 20.9. HRMS (TOF, ES+) *m/z* [M+H]⁺ calculated for C₁₆H₂₁NOCl 278.1312, found 278.1310.

8-[(4-Chlorophenyl)methyl]-8-azabicyclo[3.2.1]octan-3-one (**14**)

The title compound was synthesized according the general procedure **B** previously described using the 8,8-dimethyl-8-azoniabicyclo[3.2.1]octan-3-one iodide (**13**) and the 4-chlorobenzylamine as starting materials.

Flash chromatography cyHex to cyHex/EtOAc 85/15. Yield: 48%. ¹H-NMR (CD₂Cl₂): δ (ppm) 7.42 (d, J = 8.4 Hz, 2H), 7.35 (d, J = 8.5 Hz, 2H), 3.75 (s, 2H), 3.50 - 3.46 (m, 2H), 2.68 (dd, J = 15.7 Hz, J = 4.6 Hz, 2H), 2.22 - 2.10 (m, 4H), 1.64 - 1.61 (m, 2H). ¹³C-NMR (CD₂Cl₂): δ (ppm) 209.4, 138.4, 132.4, 129.8, 128.3, 58.7, 54.4, 48.2, 27.7. HRMS (TOF, ES+) m/z [M+H]⁺ calculated for C₁₄H₁₇NOCl 250.0999, found 250.1003.

8-[2-(4-Chlorophenyl)-1-methyl-ethyl]-8-azabicyclo[3.2.1]octan-3-one (**15**)

To a solution of 4-chlorophenylacetone (1 eq.) in DCE (C = 1.6 M) with activated molecular sieves 3 Å was added a solution of 8-azabicyclo[3.2.1]octan-3-one hydrochloride (1.1 eq.) and triethylamine (1.1 eq.) in DCE (C = 0.8 M). Acetic acid (1 eq.) and sodium triacetoxyborohydride (1.4 eq.) were then added and the resulting solution was stirred at RT for 4 hours. The solution was then basified with aqueous 1N NaOH solution and extracted with DCM (3x). The combined organic layers were washed with brine (1x), dried over MgSO₄ and concentrated under reduced pressure. The residue was purified by flash chromatography (cyHex to cyHex/EtOAc 4/6) to give 8-[2-(4-chlorophenyl)-1-methyl-ethyl]-8-azabicyclo[3.2.1]octan-3-one (**15**). Yield: 68%. ¹H-NMR (CD₂Cl₂): δ (ppm) 7.30 (d, J = 8.5 Hz, 2H), 7.18 (d, J = 8.5 Hz, 2H), 3.93 - 3.89 (m, 1H), 3.82 - 3.77 (m, 1H), 3.08 - 2.97 (m, 2H), 2.75 - 2.52 (m, 3H), 2.20 - 2.09 (m, 2H), 2.03 - 1.97 (m, 2H), 1.65 - 1.59 (m, 3H), 1.04 (d, J = 6.5 Hz, 3H). ¹³C-NMR (CD₂Cl₂): δ (ppm) 209.4, 138.3, 131.7, 131.0, 128.2, 56.2, 55.1, 52.4, 45.8, 45.6, 41.4, 28.9, 28.4, 17.9. HRMS (TOF, ES+) m/z [M+H]⁺ calculated for C₁₆H₂₁NOCl 278.1312, found 278.1310.

2 steps procedure for the synthesis of 8-[2-(4-chlorophenyl)acetyl]-8-azabicyclo[3.2.1]octan-3-one (**17**).

1-(Benzotriazol-1-yl)-2-(4-chlorophenyl)ethanone (**16**)

1H-benzotriazole (3 eq.) and SOCl₂ (1 eq.) in DCM (C = 1 M) were added dropwise to a solution of 2-(4-chlorophenyl)acetic acid (1 eq.) in DCM (C = 1 M). The reaction mixture was stirred for 24 hours at RT. The precipitate was filtered off and the filtrate was concentrated under vacuum. The residue was purified by flash chromatography (cyHex to cyHex/DCM 8/2) to give 1-(benzotriazol-1-yl)-2-(4-chlorophenyl)ethanone (**16**). Yield : 74%. ¹H-NMR (CD₂Cl₂): δ (ppm) 8.28 (dt, J = 8.2 Hz, J = 0.9 Hz, 1H), 8.16 (dt, J = 8.3 Hz, J = 0.9 Hz, 1H), 7.70 (ddd, J = 8.2 Hz, J = 7.2 Hz, J = 1.1 Hz, 1H), 7.56 (ddd, J = 8.3 Hz, J = 7.2 Hz, J = 1.1 Hz, 1H), 7.43 (d, J = 8.5 Hz, 2H), 7.38 (d, J = 8.7 Hz, 2H), 4.74 (s, 2H).

8-[2-(4-Chlorophenyl)acetyl]-8-azabicyclo[3.2.1]octan-3-one (**17**)

Nortropinone hydrochloride (1.1 eq.) and DMAP (1.1 eq.) were stirred in chloroform (C = 0.3 M) for 5 minutes at RT. Then, 1-(benzotriazol-1-yl)-2-(4-chlorophenyl)ethanone (**16**, 1 eq.) was added and the solution was heated under microwave irradiation for 15 minutes at 100 °C. The resulting solution was washed with aqueous saturated Na₂CO₃ (3x), HCl_{aq} 1N (3x) and brine (1x). The organic phase was dried over MgSO₄ and concentrated to dryness to afford 8-[2-(4-chlorophenyl)acetyl]-8-azabicyclo[3.2.1]octan-3-one (**17**). Yield: 81%. ¹H-NMR (CD₂Cl₂): δ (ppm) 7.36 (d, J = 8.6 Hz, 2H), 7.28 (d, J = 8.6 Hz, 2H), 4.95 - 4.91 (m, 1H), 4.52 - 4.48 (m, 1H), 3.80 (d, J = 15.1 Hz, 1H), 3.70 (d, J = 15.1 Hz, 1H), 2.69 (dd, J = 16.0 Hz, J = 4.7 Hz, 1H), 2.40 - 2.32 (m, 3H), 2.17 - 2.0 (m, 2H), 1.82 - 1.67 (m, 2H). ¹³C-NMR (CD₂Cl₂): δ (ppm) 206.7, 166.7, 133.7, 132.7, 130.4, 128.7, 54.2, 51.1, 49.4, 48.7, 40.5, 29.9, 27.8. HRMS (TOF, ES+) m/z [M+H]⁺ calculated for C₁₅H₁₇NO₂Cl 278.0948, found 278.0946.

8-[2-(4-Chlorophenyl)ethyl]-3-(difluoromethylene)-8-azabicyclo[3.2.1]octane (**18**)

Under argon atmosphere, potassium tert-butoxide (2.2 eq.) dissolved in dry DMF (C = 0.9 M) was added to a solution of 8-[2-(4-chlorophenyl)ethyl]-8-azabicyclo[3.2.1]octan-3-one (**1**, 1.2 eq.) and 2-

(difluoromethylsulfonyl)pyridine (1 eq.) in dry DMF (C = 0.25 M) at -50 °C. The reaction mixture was allowed to warm up to -25 °C. The mixture was stirred for 4 days at -25 °C. Then, the reaction mixture was quenched with aqueous saturated NH₄Cl (C = 0.5 M), followed by HCl 3 M (C = 0.5 M). The reaction mixture was allowed to warm up to RT. A solution of NaOH 3 M (C = 0.5 M) was added and the product was extracted with DCM (3x). The combined organic layers were dried over MgSO₄ and concentrated in vacuo. The residue was purified by flash chromatography (cyHex to cyHex/EtOAc 9/1) to give 8-[2-(4-chlorophenyl)ethyl]-3-(difluoromethylene)-8-azabicyclo[3.2.1]octane (**18**). Yield: 30%. ¹H-NMR (CD₂Cl₂): δ (ppm) 7.31 (d, *J* = 8.6 Hz, 2H), 7.24 (d, *J* = 8.4 Hz, 2H), 3.54 - 3.46 (m, 2H), 2.97 - 2.92 (m, 2H), 2.79 - 2.74 (m, 2H), 2.53 - 2.49 (m, 2H), 2.16 (dd, *J* = 15.2 Hz, *J* = 1.1 Hz, 2H), 2.04 - 1.99 (m, 2H), 1.61 (d, *J* = 8.0 Hz, 2H). ¹³C-NMR (CD₂Cl₂): δ (ppm) 153.3 (t, *J* = 288.3 Hz), 138.3, 131.8, 130.2, 128.4, 81.4 (t, *J* = 18.9 Hz), 59.2, 50.0, 33.8, 29.2, 26.3. HRMS (TOF, ES+) *m/z* [M+H]⁺ calculated for C₁₆H₁₉NF₂Cl 298.1174, found 298.1172.

8'-[2-(4-Chlorophenyl)ethyl]spiro[1,3-dioxolane-2,3'-8-azabicyclo[3.2.1]octane] (**19**)

To a solution of 8-[2-(4-chlorophenyl)ethyl]-8-azabicyclo[3.2.1]octan-3-one (**1**, 1 eq.) in dry MeCN (C = 0.15 M) under an argon stream was added ethanediol (2.2 eq.) followed by chlorotrimethylsilane (4.4 eq.). The reaction mixture was heated under microwave irradiation for 25 minutes at 80 °C. Then a saturated solution of NaHCO₃ was added and the resulting kksolution was extracted with DCM (3x). The combined organic layer were washed with brine (1x), dried over MgSO₄ and concentrated to dryness to give 8'-[2-(4-chlorophenyl)ethyl]spiro[1,3-dioxolane-2,3'-8-azabicyclo[3.2.1]octane] (**19**). Yield: 83%. ¹H-NMR (CD₂Cl₂): δ (ppm) 7.28 (d, *J* = 8.5 Hz, 2H), 7.21 (d, *J* = 8.5 Hz, 2H), 3.95 (t, *J* = 6.2 Hz, 2H), 3.79 (t, *J* = 6.5 Hz, 2H), 3.33 - 3.28 (m, 2H), 2.83 - 2.75 (m, 2H), 2.70 - 2.64 (m, 2H), 2.0 - 1.94 (m, 4H), 1.92 - 1.83 (m, 2H), 1.67 (d, *J* = 13.6 Hz, 2H). ¹³C-NMR (CD₂Cl₂): δ (ppm) 139.4, 131.5, 130.2, 128.2, 107.2, 64.2, 62.9, 58.5, 39.8, 34.9, 29.7, 25.7. HRMS (TOF, ES+) *m/z* [M+H]⁺ calculated for C₁₇H₂₃NO₂Cl 308.1417, found 308.1419.

8-[2-(4-Chlorophenyl)ethyl]-3,3-dimethoxy-8-azabicyclo[3.2.1]octane (**20**)

Under argon atmosphere, trimethylorthoformate (5 eq.) was added to a solution of 8-[2-(4-chlorophenyl)ethyl]-8-azabicyclo[3.2.1]octan-3-one (**1**, 1 eq.) and PTSA (2 eq.) in dry MeOH (C = 0.5 M). The reaction mixture was heated under microwave irradiation for 25 minutes at 80 °C. Then a saturated solution of NaHCO₃ was added and the resulting solution was extracted with DCM (3x). The combined organic layers were dried over MgSO₄ and concentrated under vacuum. The residue was purified by flash chromatography (cyHex to cyHex/[EtOAc/MeOH 3/1]) to yield 8-[2-(4-chlorophenyl)ethyl]-3,3-dimethoxy-8-azabicyclo[3.2.1]octane (**20**). Yield: 60%. ¹H-NMR (CD₂Cl₂): δ (ppm) 7.29 (d, *J* = 8.6 Hz, 2H), 7.21 (d, *J* = 8.6 Hz, 2H), 3.27 - 3.21 (m, 2H), 3.16 (s, 3H), 3.11 (s, 3H), 2.78 - 2.73 (m, 2H), 2.66 - 2.60 (m, 2H), 1.92 - 1.86 (m, 2H), 1.81 - 1.73 (m, 6H). ¹³C-NMR (CD₂Cl₂): δ (ppm) 139.7, 131.3, 130.2, 128.2, 98.9, 57.9, 52.7, 47.9, 46.8, 37.1, 35.2, 25.8. HRMS (TOF, ES+) *m/z* [M+H]⁺ calculated for C₁₇H₂₅NO₂Cl 310.1574, found 310.1569.

8-(2-Phenylethyl)-8-azabicyclo[3.2.1]octan-3-one (**21**)

The title compound was synthesized according the general procedure **B** previously described using the 8,8-dimethyl-8-azoniabicyclo[3.2.1]octan-3-one iodide (**13**) and 2-phenylethylamine as starting materials. Yield: 54%. ¹H-NMR (CD₂Cl₂): δ (ppm) 7.34 - 7.19 (m, 5H), 3.61 - 3.55 (m, 2H), 2.91 - 2.80 (m, 4H), 2.66 (dd, *J* = 16.0 Hz, *J* = 4.5 Hz, 2H), 2.19 - 2.13 (m, 2H), 2.06 - 2.01 (m, 2H), 1.63 - 1.55 (m,

2H). **¹³C-NMR** (CD₂Cl₂): δ (ppm) 209.5, 140.6, 128.7, 128.3, 126.0, 58.8, 52.3, 47.4, 35.9, 27.9. **HRMS** (TOF, ES+) m/z [M+H]⁺ calculated for C₁₅H₂₀NO 230.1545, found 230.1546.

8-[2-(3,4-Dichlorophenyl)ethyl]-8-azabicyclo[3.2.1]octan-3-one (**22**)

The title compound was synthesized according the general procedure **B** previously described using the 8,8-dimethyl-8-azoniabicyclo[3.2.1]octan-3-one iodide (**13**) and 3,4-dichlorophenylethylamine as starting materials. Yield: 60%. **¹H-NMR** (CD₂Cl₂): δ (ppm) 7.41 - 7.39 (d, *J* = 8.2 Hz, 1H), 7.41 (d, *J* = 2.1 Hz, 1H), 7.17-7.13 (dd, *J* = 8.2 Hz, *J* = 2.1 Hz, 1H), 3.53 (m, 2H), 2.82 (s, 4H), 2.65 - 2.59 (dd, *J* = 15.91 Hz, *J* = 4.30 Hz, 2H), 2.19 - 2.13 (m, 2H), 2.05 - 2.01 (m, 2H), 1.63 - 1.56 (m, 2H). **¹³C-NMR** (CD₂Cl₂): δ (ppm) 209.3, 141.2, 131.8, 130.7, 130.1, 129.7, 128.5, 58.9, 51.9, 47.6, 35.0, 27.8. **HRMS** (TOF, ES+) m/z [M+H]⁺ calculated for C₁₅H₁₈NOCl₂ 298.0765, found 298.0768.

8-[2-(2,4-Dichlorophenyl)ethyl]-8-azabicyclo[3.2.1]octan-3-one (**23**)

The title compound was synthesized according the general procedure **B** previously described using the 8,8-dimethyl-8-azoniabicyclo[3.2.1]octan-3-one iodide (**13**) and 2,4-dichlorophenylethylamine as starting materials. Yield: 32%. **¹H-NMR** (CD₂Cl₂): δ (ppm) 7.41 (d, *J* = 2.0 Hz, 1H), 7.29 (d, *J* = 8.2 Hz, 1H), 7.23 (dd, *J* = 8.2 Hz, *J* = 2.0 Hz, 1H), 3.59 - 3.55 (m, 2H), 3.0 - 2.94 (m, 2H), 2.83 - 2.77 (m, 2H), 2.64 (dd, *J* = 16.0 Hz, *J* = 4.5 Hz, 2H), 2.16 (d, *J* = 15.9 Hz, 2H), 2.06 - 2.01 (m, 2H), 1.58 (d, *J* = 7.9 Hz, 2H). **¹³C-NMR** (CD₂Cl₂): δ (ppm) 209.3, 136.8, 134.6, 132.3, 131.9, 129.0, 127.0, 59.0, 50.4, 47.6, 33.1, 27.8. **HRMS** (TOF, ES+) m/z [M+H]⁺ calculated for C₁₅H₁₈NOCl₂ 298.0765, found 298.0764.

8-[2-(4-Pyridyl)ethyl]-8-azabicyclo[3.2.1]octan-3-one (**24**)

The title compound was synthesized according the general procedure **B** previously described using the 8,8-dimethyl-8-azoniabicyclo[3.2.1]octan-3-one iodide (**13**) and 4-(2-aminoethyl)pyridine as starting materials. Flash chromatography cyHex to cyHex/(EtOAc-MeOH 3/1) 75/25. Yield: 64%. **¹H-NMR** (CD₂Cl₂): δ (ppm) 8.49 (d, *J* = 4.3 Hz, 2H), 7.22 (d, *J* = 4.2 Hz, 2H), 3.57 - 3.52 (m, 2H), 2.86 (s, 4H), 2.66 - 2.59 (dd, *J* = 15.9 Hz, *J* = 4.4 Hz, 2H), 2.19 - 2.13 (m, 2H), 2.06 - 2.01 (m, 2H), 1.63 - 1.56 (m, 2H). **¹³C-NMR** (CD₂Cl₂): δ (ppm) 209.3, 149.5, 133.3 (HMBC coupling), 124.2, 58.9, 51.2, 47.6, 35.1, 27.8. **HRMS** (TOF, ES+) m/z [M+H]⁺ calculated for C₁₄H₁₉N₂O 231.1497, found 231.1502.

8-[2-(p-Tolyl)ethyl]-8-azabicyclo[3.2.1]octan-3-one (**25**)

The title compound was synthesized according the general procedure **B** previously described using the 8,8-dimethyl-8-azoniabicyclo[3.2.1]octan-3-one iodide (**13**) and 2-(4-methylphenyl)ethylamine as starting materials. Flash chromatography cyHex to cyHex/EtOAc 8/2. Yield: 59%. **¹H-NMR** (CD₂Cl₂): δ (ppm) 7.17 - 7.10 (m, 4H), 3.58 - 3.45 (m, 2H), 2.95 - 2.82 (m, 4H), 2.69 (dd, *J* = 16 Hz, *J* = 5.2 Hz, 2H), 2.34 (s, 3H), 2.18 - 2.12 (m, 2H), 2.06 - 2.00 (m, 2H), 1.62 - 1.55 (m, 2H). **¹³C-NMR** (CD₂Cl₂): δ (ppm) 209.5, 137.4, 135.6, 128.9, 128.6, 58.8, 52.4, 47.3, 35.4, 27.9, 20.7. **HRMS** (TOF, ES+) m/z [M+H]⁺ calculated for C₁₆H₂₂NO 244.1701, found 244.1703.

8-[2-(4-Methoxyphenyl)ethyl]-8-azabicyclo[3.2.1]octan-3-one (**26**)

The title compound was synthesized according the general procedure **B** previously described using the 8,8-dimethyl-8-azoniabicyclo[3.2.1]octan-3-one iodide (**13**) and 2-(4-methoxyphenyl)ethylamine as starting materials. Flash chromatography cyHex to cyHex/EtOAc 8/2. Yield: 59%. **¹H-NMR** (CD₂Cl₂): δ (ppm) 7.20 (d, *J* = 8.7 Hz, 2H), 6.87 (d, *J* = 8.7 Hz, 2H), 3.80 (s, 3H), 3.61 - 3.56 (m, 2H), 2.81 (s, 4H), 2.66 (dd, *J* = 15.8 Hz, *J* = 4.3 Hz, 2H), 2.17 (d, *J* = 15.6 Hz, 2H), 2.08 - 2.0 (m, 2H), 1.60 (d, *J* = 7.9 Hz,

2H). ¹³C-NMR (CD₂Cl₂): δ (ppm) 209.6, 158.0, 132.5, 129.6, 113.6, 58.8, 55.1, 52.5, 47.4, 35.0, 27.9. HRMS (TOF, ES+) m/z [M+H]⁺ calculated for C₁₆H₂₂NO₂ 260.1651, found 260.1649.

8-[2-(4-Fluorophenyl)ethyl]-8-azabicyclo[3.2.1]octan-3-one (**27**)

The title compound was synthesized according the general procedure **B** previously described using the 8,8-dimethyl-8-azoniabicyclo[3.2.1]octan-3-one iodide (**13**) and 2-(4-fluorophenyl)ethylamine as starting materials. Flash chromatography cyHex to cyHex/EtOAc 6/4. Yield: 51%. ¹H-NMR (CD₂Cl₂): δ (ppm) 7.25 (dd, *J* = 5.6 Hz, *J* = 8.7 Hz, 2H), 7.0 (t, *J* = 9 Hz, 2H), 3.57 - 3.54 (m, 2H), 2.88 - 2.77 (m, 4H), 2.63 (dd, *J* = 16.0 Hz, *J* = 4.6 Hz, 2H), 2.16 (d, *J* = 15.7 Hz, 2H), 2.06 - 2.00 (m, 2H), 1.63 - 1.55 (m, 2H). ¹³C-NMR (CD₂Cl₂): δ (ppm) 209.4, 161.4 (d, *J* = 242 Hz), 136.4 (d, *J* = 3 Hz), 130.2 (d, *J* = 7.8 Hz), 114.9 (d, *J* = 21 Hz), 58.9, 52.4, 47.5, 35.1, 27.8. HRMS (TOF, ES+) m/z [M+H]⁺ calculated for C₁₅H₁₉NOF 248.1451, found 248.1448.

8-[2-(4-Bromophenyl)ethyl]-8-azabicyclo[3.2.1]octan-3-one (**28**)

The title compound was synthesized according the general procedure **B** previously described using the 8,8-dimethyl-8-azoniabicyclo[3.2.1]octan-3-one iodide (**13**) and 2-(4-bromophenyl)ethylamine as starting materials. Flash chromatography cyHex to cyHex/EtOAc 8/2. Yield: 64%. ¹H-NMR (CD₂Cl₂): δ (ppm) 7.44 (d, *J* = 8.4 Hz, 2H), 7.18 (d, *J* = 8.4 Hz, 2H), 3.56 - 3.53 (m, 2H), 2.86 - 2.82 (m, 4H), 2.63 (dd, *J* = 15.9 Hz, *J* = 4.3 Hz, 2H), 2.19 - 2.12 (m, 2H), 2.05 - 2.01 (m, 2H), 1.62 - 1.55 (m, 2H). ¹³C-NMR (CD₂Cl₂): δ (ppm) 208.5, 139.8, 131.7, 130.9, 119.7, 59.0, 52.2, 47.4, 35.3, 27.8. HRMS (TOF, ES+) m/z [M+H]⁺ calculated for C₁₅H₁₉NOBr 308.0650, found 308.0656.

8-[2-(4-Nitrophenyl)ethyl]-8-azabicyclo[3.2.1]octan-3-one (**29**)

The title compound was synthesized according the general procedure **B** previously described using the 8,8-dimethyl-8-azoniabicyclo[3.2.1]octan-3-one iodide (**13**) and 2-(4-nitrophenyl)ethylamine as starting materials. Yield: 45%. ¹H-NMR (CD₂Cl₂): δ (ppm) 8.17 (d, *J* = 8.7 Hz, 2H), 7.46 (d, *J* = 8.7 Hz, 2H), 3.57 - 3.52 (m, 2H), 3.0 - 2.95 (m, 2H), 2.90 - 2.84 (m, 2H), 2.62 (dd, *J* = 16.1 Hz, *J* = 4.4 Hz, 2H), 2.17 (d, *J* = 16.1 Hz, 2H), 2.06 - 2.00 (m, 2H), 1.58 (d, *J* = 8.7 Hz, 2H). ¹³C-NMR (CD₂Cl₂): δ (ppm) 209.2, 148.7, 129.7, 123.4, 121.1 (HMBC coupling), 59.0, 61.7, 47.6, 35.6, 27.8. HRMS (TOF, ES+) m/z [M+H]⁺ calculated for C₁₅H₁₉N₂O₃ 275.1396, found 275.1401.

8-[2-[4-(Trifluoromethyl)phenyl]ethyl]-8-azabicyclo[3.2.1]octan-3-one (**30**)

The title compound was synthesized according the general procedure **B** previously described using the 8,8-dimethyl-8-azoniabicyclo[3.2.1]octan-3-one iodide (**13**) and 2-(4-trifluoromethylphenyl)ethylamine as starting materials. Yield: 26%. ¹H-NMR (CD₂Cl₂): δ (ppm) 7.59 (d, *J* = 8.0 Hz, 2H), 7.42 (d, *J* = 7.8 Hz, 2H), 3.58 - 3.54 (m, 2H), 2.97 - 2.91 (m, 2H), 2.88 - 2.83 (m, 2H), 2.64 (dd, *J* = 16.0 Hz, *J* = 4.6 Hz, 2H), 2.17 (d, *J* = 16.7 Hz, 2H), 2.07 - 2.02 (m, 2H), 1.64 - 1.56 (m, 2H). ¹³C-NMR (CD₂Cl₂): δ (ppm) 209.3, 145.0, 129.2, 128.1 (q, *J* = 31.7 Hz), 125.1 (q, *J* = 3.7 Hz), 124.4 (q, *J* = 271.5 Hz), 58.9, 51.9, 47.5, 35.7, 27.8. HRMS (TOF, ES+) m/z [M+H]⁺ calculated for C₁₆H₁₉NOF₃ 298.1419, found 298.1422.

8-[2-[3-(Trifluoromethyl)phenyl]ethyl]-8-azabicyclo[3.2.1]octan-3-one (**31**)

The title compound was synthesized according the general procedure **B** previously described using the 8,8-dimethyl-8-azoniabicyclo[3.2.1]octan-3-one iodide (**13**) and 2-(3-trifluoromethylphenyl)ethylamine as starting materials. Flash chromatography cyHex to cyHex/EtOAc

75/25. Yield: 25%. ¹H-NMR (CD₂Cl₂): δ (ppm) 7.56 (s, 1H), 1.53 - 7.43 (m, 3H), 3.58 - 3.54 (m, 2H), 3.0 - 2.91 (m, 2H), 2.88 - 2.83 (m, 2H), 2.64 (dd, *J* = 16.1 Hz, *J* = 4.1 Hz, 2H), 2.16 (d, *J* = 16.1 Hz, 2H), 2.07 - 2.01 (m, 2H), 1.58 (d, *J* = 7.9 Hz, 2H). ¹³C-NMR (CD₂Cl₂): δ (ppm) 209.2, 141.6, 132.4, 130.2 (q, *J* = 31.6 Hz), 128.7, 125.5 (q, *J* = 3.7 Hz), 124.4 (q, *J* = 272 Hz), 122.8 (q, *J* = 3.8 Hz), 58.9, 52.0, 47.5, 35.6, 27.8. HRMS (TOF, ES+) *m/z* [M+H]⁺ calculated for C₁₆H₁₉NOF₃ 298.1419, found 298.1420.

8-[2-[2-(Trifluoromethyl)phenyl]ethyl]-8-azabicyclo[3.2.1]octan-3-one (**32**)

The title compound was synthesized according the general procedure **B** previously described using the 8,8-dimethyl-8-azoniabicyclo[3.2.1]octan-3-one iodide (**13**) and 2-(2-trifluoromethylphenyl)ethylamine as starting materials. Flash chromatography cyHex to cyHex/(EtOAc-EtOH 3-1) 9/1. Yield: 25%. ¹H-NMR (CD₂Cl₂): δ (ppm) 7.67 (d, *J* = 7.9 Hz, 1H), 7.54 (t, *J* = 7.9 Hz, 1H), 7.47 (d, *J* = 7.4 Hz, 1H), 7.36 (t, *J* = 7.4 Hz, 1H), 3.63 - 3.57 (m, 2H), 3.08 - 3.03 (m, 2H), 2.85 - 2.79 (m, 2H), 2.65 (dd, *J* = 16.1 Hz, *J* = 4.4 Hz, 2H), 2.18 (dd, *J* = 17.1 Hz, *J* = 1.8 Hz, 2H), 2.07 - 2.00 (m, 2H), 1.6 (d, *J* = 8.0 Hz, 2H). ¹³C-NMR (CD₂Cl₂): δ (ppm) 209.4, 138.9, 131.8, 131.7, 128.3 (q, *J* = 29.9 Hz), 126.3, 125.9 (q, *J* = 4.7 Hz), 124.6 (q, *J* = 274.0 Hz), 59.0, 52.4, 47.6, 32.7, 27.8. HRMS (TOF, ES+) *m/z* [M+H]⁺ calculated for C₁₆H₁₉NOF₃ 298.1419, found 298.1417.

4.2. Crystallography

Protein production and purification were performed as previously reported [7]. Crystals in orthorhombic space group P2₁2₁2₁ were obtained in several conditions, with the best conditions being hanging drop vapor diffusion technique at 20 °C and 200 mM ammonium chloride, 100 mM MES pH 6.0, 20% (w/v) PEG6000, as crystallization buffer. In addition, EthR2 crystals in monoclinic space group C121 were produced by changing imidazole concentration of the protein sample from 100 to 400 mM and by ranging the pH and the ammonium chloride concentration of crystallization buffer in 6.0-7.0 and 200-400 mM, respectively. Crystals were then transferred to a new drop for soaking experiments with small molecules at 1.0 mM concentration for 1-3 days at 20 °C. Molecules **9** and **30** were solved by co-crystallization, as attempts to soak EthR2 crystals with these molecules failed. In that cases the following procedure was applied: a diluted protein sample (60 μM) was incubated at 4 °C for overnight with 1 mM compound (protein:/compound molar ratio 6/100 and DMSO final concentration of 5% (v/v)); the solution was then concentrated to ~10 mg/ml protein concentration and screened for crystallization with the initial crystallographic conditions of orthorhombic form.

The X-ray diffraction data were collected in-house or using synchrotron radiation facilities at ESRF-ID30A-1 (Grenoble, France) and at SOLEIL-PX1 (Paris, France). Data indexations were automatically performed with autoProc or XDSME, both based on the XDS program.[27] Data collection statistics are provided in Table 6. Structures were solved by molecular replacement with MOLREP [28] using as searching template the PDB ID 5N7O [15]. Structure refinements were done without non-crystallographic symmetry restraints by iteratively cycling through REFMAC5 [29] and COOT [30]. Stereochemical description and restraints for small molecules were produced using AceDRG [31] from the SMILES string and the initial ligand pose was set up using the FINDLIGAND tool of the CCP4 software suite. In each solved crystal structures, ligands were modeled and refined at full occupancy. The fit between modeled ligand and electron density was assessed with EDSTATS [32], using four local metrics, the real-space R-factor (RSR), the real-space correlation coefficient (RSCC), the real-space Z-difference score (RSZD) and the real-space Z-observed score (RSZO). Final refinement

statistics are given in Table 6 using MolProbity [33]. The refined coordinates and the structure factors were deposited in the Protein Data Bank under the PDB IDs indicated in Table 6.

compound	1	2	3	4	5	9	30
PDB ID	6HRW	6HRX	6HRY	6HRZ	6HS0	6HS1	6HS2
Structure ID	BDM14272	BDM72201	BDM72719	BDM72170	BDM71847	BDM76060	BDM76150
Data collection statistics							
Beamline	Rigaku MicroMax-007	SOLEIL/PX1	SOLEIL/PX1	ESRF/MASSIF -1	ESRF/MASSIF -1	ESRF/MASSIF -1	ESRF/MASSIF -1
Detector type	Saturn944+	Pilatus 6M	Pilatus 6M	Pilatus3 2M	Pilatus3 2M	Pilatus3 2M	Pilatus3 2M
Wavelength (Å)	1.541870	0.97857	0.97857	0.96600	0.96600	0.96600	0.96600
Autoprocessing software	XDSME	XDSME	XDSME	autoProc	autoProc	autoProc	autoProc
Space group	P2 ₁ 2 ₁ 2 ₁	P2 ₁ 2 ₁ 2 ₁	P2 ₁ 2 ₁ 2 ₁	C121	C121	P2 ₁ 2 ₁ 2 ₁	P2 ₁ 2 ₁ 2 ₁
a, b, c (Å)	59.81; 74.57; 88.78	59.54; 74.15; 91.58	59.52; 75.09; 88.48	109.91; 40.72; 108.93	110.09; 40.56; 108.74	59.46; 74.01; 91.65	59.48; 73.57; 91.10
α, β, γ (°)	90.00; 90.00; 90.00	90.00; 90.00; 90.00	90.00; 90.00; 90.00	90.00; 95.67; 90.00	90.00; 96.75; 90.00	90.00; 90.00; 90.00	90.00; 90.00; 90.00
Resolution range (Å)	30.00-2.45 (2.60-2.45)	50.00-1.87 (1.98-1.87)	50.00-1.84 (1.95-1.84)	54.69-1.57 (1.61-1.57)	107.99-1.45 (1.48-1.45)	57.58-1.69 (1.72-1.69)	49.80-1.87 (1.90-1.87)
No. of unique reflections	15012 (2334)	34087 (5344)	34594 (5290)	66857 (4922)	80773 (4071)	45240 (2215)	33585 (1659)
Multiplicity	6.99 (6.57)	5.41 (5.36)	5.37 (5.34)	3.1 (2.9)	2.7 (2.4)	4.6 (4.8)	4.9 (4.6)
Completeness (%)	99.4 (97.5)	99.5 (98.2)	98.9 (95.2)	98.7 (99.0)	95.4 (98.3)	99.0 (98.8)	99.5 (99.5)
mean I/σ(I)	9.65 (2.04)	20.66 (2.92)	18.34 (2.35)	16.98 (2.37)	13.95 (2.23)	14.25 (2.17)	17.12 (1.95)
R _{meas} (%)	23.5 (120.3)	4.8 (61.4)	6.1 (66.3)	4.0 (54.8)	4.5 (57.0)	5.6 (82.7)	5.2 (86.9)
V _m (Å ³ Da ⁻¹)	2.05	2.10	2.05	2.52	2.50	2.09	2.07
Solvent content (%)	40.17	41.41	40.10	51.17	50.88	41.27	40.58
Refinement statistics (MolProbity)							
Number of refined atoms protein/ligand/water	2914/18/9	2910/28/27	2961/28/54	3030/26/159	3037/28/240	2914/19/85	2914/21/41
Final Rwork/Rfree (%)	22.14/26.98	22.49/26.08	21.34/24.24	21.26/23.03	20.30/21.77	22.38/25.50	24.33/22.60
RMSD bond lengths (Å)	0.0149	0.0149	0.0151	0.0156	0.0149	0.0144	0.0141
RMSD bond angles (°)	2.01	1.79	1.80	1.89	1.87	1.76	1.76
Overall mean B factor (Å ²) protein/ligand/water	35.1/57.1/23.1	37.3/52.5/33.9	32.6/36.6/34.0	26.5/26.5/30.1	21.1/25.2/28.2	33.8/41.1/34.9	39.3/44.7/38.1
Rama favored/outliers (%)	99.47/0.26	100.00/0.00	100.00/0.00	99.75/0.00	100.00/0.00	100.00/0.00	99.74/0.00
Clashscore (percentile)	5.26 (99th)	4.74 (97th)	3.66 (98th)	3.42 (98th)	2.43 (99th)	3.56 (98th)	4.06 (98th)
MolProbity score (percent)	1.47 (99th)	1.20 (99th)	1.17 (99th)	1.13 (99th)	1.03 (99th)	1.15 (99th)	1.19 (99th)
Ligand RSR/RSCC	0.120/0.887	0.109/0.929	0.097/0.922	0.070/0.970	0.0835/0.943	0.102/0.923	0.074/0.954
Ligand RSZD/RSZO	0.763/1.779	0.791/2.140	0.692/2.68	0.843/3.936	1.114/3.861	0.493/2.262	0.603/3.072

Table 6 : crystallographic data

4.3. Biology

4.3.1 Thermal Shift Assay on EthR2 (screening conditions)

60 nL of each fragment at 100 mM in DMSO was dispensed in a 384-well plate using the Echo[®]550 liquid handler (LabCyte). The recombinant *M. tuberculosis* protein EthR2 (Rv0078) was used at a final concentration of 20 μM. The fluorescent dye NanoOrange[®] (Life technologies) was used to monitor EthR2 unfolding. This dye is environmentally sensitive and leads to an increase in fluorescence following exposure of hydrophobic regions during protein unfolding. The final sample concentration in a total assay volume of 6.06 μL was 20 μM EthR2, 3x NanoOrange[®], 1.6% DMSO, and 1 mM fragment in the Thermal Shift Assay-buffer (100 mM Glycine, pH 7, 150 mM NaCl). The thermal shift assay was conducted in a Lightcycler 480 (Roche). The system contained a heating/cooling device for temperature control and a charge-coupled device (CCD) detector for real-time imaging of the fluorescence changes in the wells of the microplate. The samples were heated from 37 to 85 °C with a heating rate of 0.05 °C/s. The fluorescence intensity was measured at Ex/Em = 465/510 nm. The LightCycler[®] exported .ixo files were processed using the protein melting analysis tool (Roche). The output was a .csv file containing the inflection point (T_m).

4.3.2 Thermal Shift Assay on EthR2 (SAR conditions)

Compounds in DMSO were dispensed in a 96-well plate. The recombinant *M. tuberculosis* protein EthR2 (Rv0078) was used at a final concentration of 10 μM. The fluorescent dye SYPRO[®] Orange (SigmaAldrich) was used to monitor EthR2 unfolding. This dye is environmentally sensitive and leads to an increase in fluorescence following exposure of hydrophobic regions during protein unfolding. The thermal shift assay was conducted in a Lightcycler 480 (Roche). The system contained a heating/cooling device for temperature control and a charge-coupled device (CCD) detector for real-time imaging of the fluorescence changes in the wells of the microplate. The final sample concentration was 10 μM EthR2, 3x SYPRO[®] Orange, 1% DMSO, and 20 μM ligand in the Thermal Shift Assay-buffer (100 mM Glycine, pH 7, 150 mM NaCl). The samples were heated from 37 to 85 °C with a heating rate of 0.04 °C/s. The fluorescence intensity was measured at Ex/Em = 465/510 nm. The LightCycler[®] exported ixo files that were processed using the protein melting analysis tool (Roche). The output was a csv file containing the inflection point (T_m).

4.3.3 Mammalian SEAP reporter assay

Vector design. A chimeric mammalian transcriptional regulator was constructed by fusing the coding sequence of EthR2 (Rv0078) from *Mycobacterium tuberculosis* to the *Herpes simplex* derived transactivator protein VP16. The resulting ORF was sequence optimized for expression in human/mouse, synthesized (Genscript) and introduced into pSEAP2-control (Clontech) using EcoRI/XbaI to generate the expression vector pCK289 (PSV40-EthR2-VP16-HA-pA). To enable EthR2-VP16 based transcriptional control, we designed a synthetic DNA by fusing the 61-nucleotide spanning intergenic region of *ethA2* (Rv0077c) and *ethR2* (Rv0078) upstream of a minimal variant of the human

cytomegalovirus derived promoter (PhCMVmin). This synthetic promoter was cloned into pSEAP2-basic (Clontech) by restriction (XhoI/EcoRI) and ligation to generate pCK287 (OEthR2-PhCMVmin-SEAP-pA), which enables EthR2-VP16 based control of human placental secreted alkaline phosphatase (SEAP) expression.

Cell culture. Baby hamster kidney cells (BHK-21, American Type Culture Collection CCL-10) were cultured in Dulbecco's modified Eagle's medium (DMEM, Gibco, catalog no. 41966) supplemented

with 10% (v/v) heat-inactivated fetal bovine serum (FBS, Gibco, catalog no. 10500) and 1% (v/v) penicillin/streptomycin (Gibco, catalog no. 15140) in a humidified atmosphere with 5% CO₂ at 37°C. Prior to transfection, cells from a confluent grown culture dish were split 1:2 to a new petri dish and grown for 16 hours. For transfection, 10µg of total plasmid DNA (5µg pCK287 and 5µg pCK289, ratio 1:1) were added to 1mL Opti-MEM medium (Gibco, catalog no. 11058021), mixed with 30µL MegaTran 1.0 transfection reagent (Origene, catalog no. TT200003) and incubated for 15min at room temperature. The DNA mix was transferred to the cells and incubated for 6h for plasmid uptake. The cells were washed with PBS, detached from the plate with 0.05% trypsin-EDTA (Gibco, catalog no. 25300), counted and diluted to 500.000 cells/mL using fresh culture medium. Hundred microliter of cell suspension was dispersed per well of a 96 well culture dish. Compound dilutions were prepared by adding 1.2µL compounds (10mM stock solution in DMSO) to 600µL culture medium, 1:2 dilution rows were prepared, and 100µL of compound dilutions were finally added to the cells. After incubation for 48h the SEAP expression was quantified from cell culture supernatants using a p-nitrophenyl phosphate based method.

References

- [1] Global tuberculosis report 2017. Geneva: World Health Organization., 2017.
- [2] N. Willand, B. Dirie, X. Carette, P. Bifani, A. Singhal, M. Desroses, F. Leroux, E. Willery, V. Mathys, R. Deprez-Poulain, G. Delcroix, F. Frenois, M. Aumercier, C. Loch, V. Villeret, B. Deprez, A.R. Baulard, Synthetic EthR inhibitors boost antituberculous activity of ethionamide, *Nature Med.*, 15 (2009) 537.
- [3] M. Flipo, M. Desroses, N. Lecat-Guillet, B. Dirie, X. Carette, F. Leroux, C. Piveteau, F. Demirkaya, Z. Lens, P. Rucktooa, V. Villeret, T. Christophe, H.K. Jeon, C. Loch, P. Brodin, B. Deprez, A.R. Baulard, N. Willand, Ethionamide Boosters: Synthesis, Biological Activity, and Structure-Activity Relationships of a Series of 1,2,4-Oxadiazole EthR Inhibitors, *J. Med. Chem.*, 54 (2011) 2994-3010.
- [4] M. Flipo, M. Desroses, N. Lecat-Guillet, B. Villemagne, N. Blondiaux, F. Leroux, C. Piveteau, V. Mathys, M.P. Flament, J. Siepmann, V. Villeret, A. Wohlkönig, R. Wintjens, S.H. Soror, T. Christophe, H.K. Jeon, C. Loch, P. Brodin, B. Déprez, A.R. Baulard, N. Willand, Ethionamide boosters. 2. Combining bioisosteric replacement and structure-based drug design to solve pharmacokinetic issues in a series of potent 1,2,4-oxadiazole EthR inhibitors, *J. Med. Chem.*, 55 (2012) 68-83.
- [5] J. Costa-Gouveia, E. Pancani, S. Jouny, A. Machelart, V. Delorme, G. Salzano, R. Iantomasi, C. Piveteau, C.J. Queval, O.R. Song, M. Flipo, B. Deprez, J.P. Saint-André, J. Hureauux, L. Majlessi, N. Willand, A. Baulard, P. Brodin, R. Gref, Combination therapy for tuberculosis treatment: pulmonary administration of ethionamide and booster co-loaded nanoparticles, *Sci Rep*, 7 (2017) 5390.
- [6] N.J. Tatum, J.W. Liebeschuetz, J.C. Cole, R. Frita, A. Herledan, A.R. Baulard, N. Willand, E. Pohl, New active leads for tuberculosis booster drugs by structure-based drug discovery, *Org Biomol Chem*, 15 (2017) 10245-10255.
- [7] V. Mendes, T.L. Blundell, Targeting tuberculosis using structure-guided fragment-based drug design, *Drug Discov Today*, 22 (2017) 546-554.
- [8] C. Marchetti, D.S.H. Chan, A.G. Coyne, C. Abell, Fragment-based approaches to TB drugs, *Parasitology*, 145 (2018) 184-195.
- [9] B. Villemagne, M. Flipo, N. Blondiaux, C. Crauste, S. Malaquin, F. Leroux, C. Piveteau, V. Villeret, P. Brodin, B.O. Villoutreix, O. Sperandio, S.H. Soror, A. Wohlkönig, R. Wintjens, B. Deprez, A.R. Baulard, N. Willand, Ligand efficiency driven design of new inhibitors of Mycobacterium tuberculosis transcriptional repressor EthR using fragment growing, merging, and linking approaches, *J Med Chem*, 57 (2014) 4876-4888.
- [10] S. Surade, N. Ty, N. Hengrung, B. Lechartier, S.T. Cole, C. Abell, T.L. Blundell, A structure-guided fragment-based approach for the discovery of allosteric inhibitors targeting the lipophilic binding site of transcription factor EthR, *Biochem J*, 458 (2014) 387-394.
- [11] P.O. Nikiforov, S. Surade, M. Blaszczyk, V. Delorme, P. Brodin, A.R. Baulard, T.L. Blundell, C. Abell, A fragment merging approach towards the development of small molecule inhibitors of Mycobacterium tuberculosis EthR for use as ethionamide boosters, *Org. Biomol. Chem.*, 14 (2016) 2318-2326.
- [12] P.O. Nikiforov, M. Blaszczyk, S. Surade, H.I. Boshoff, A. Sajid, V. Delorme, N. Deboosere, P. Brodin, A.R. Baulard, C.E. Barry, T.L. Blundell, C. Abell, Fragment-Sized EthR Inhibitors Exhibit Exceptionally Strong Ethionamide Boosting Effect in Whole-Cell Mycobacterium tuberculosis Assays, *ACS Chem Biol*, 12 (2017) 1390-1396.
- [13] D.S. Chan, V. Mendes, S.E. Thomas, B.N. McConnell, D. Matak-Vinković, A.G. Coyne, T.L. Blundell, C. Abell, Fragment Screening against the EthR-DNA Interaction by Native Mass Spectrometry, *Angew Chem Int Ed Engl*, 56 (2017) 7488-7491.
- [14] N. Blondiaux, M. Moune, M. Desroses, R. Frita, M. Flipo, V. Mathys, K. Soetaert, M. Kiass, V. Delorme, K. Djaout, V. Trebosc, C. Kemmer, R. Wintjens, A. Wohlkönig, R. Antoine, L. Huot, D. Hot, M. Coscolla, J. Feldmann, S. Gagneux, C. Loch, P. Brodin, M. Gitzinger, B. Déprez, N. Willand, A.R. Baulard, Reversion of antibiotic resistance in Mycobacterium tuberculosis by spiroisoxazoline SMART-420, *Science*, 355 (2017) 1206-1211.

- [15] A. Wohlkönig, H. Remaut, M. Moune, A. Tanina, F. Meyer, M. Desroses, J. Steyaert, N. Willand, A.R. Baulard, R. Wintjens, Structural analysis of the interaction between spiroisoxazoline SMART-420 and the Mycobacterium tuberculosis repressor EthR2, *Biochem Biophys Res Commun*, 487 (2017) 403-408.
- [16] M.C. Lo, A. Aulabaugh, G. Jin, R. Cowling, J. Bard, M. Malamas, G. Ellestad, Evaluation of fluorescence-based thermal shift assays for hit identification in drug discovery, *Anal Biochem*, 332 (2004) 153-159.
- [17] C.H. Luan, S.H. Light, S.F. Dunne, W.F. Anderson, Ligand screening using fluorescence thermal shift analysis (FTS), *Methods Mol Biol*, 1140 (2014) 263-289.
- [18] M. Flipo, N. Willand, N. Lecat-Guillet, C. Hounsou, M. Desroses, F. Leroux, Z. Lens, V. Villeret, A. Wohlkönig, R. Wintjens, T. Christophe, H. Kyoung Jeon, C. Loch, P. Brodin, A.R. Baulard, B. Déprez, Discovery of novel N-phenylphenoxyacetamide derivatives as EthR inhibitors and ethionamide boosters by combining high-throughput screening and synthesis, *J. Med. Chem.*, 55 (2012) 6391-6402.
- [19] W. Weber, R. Schoenmakers, B. Keller, M. Gitzinger, T. Grau, M. Daoud-El Baba, P. Sander, M. Fussenegger, A synthetic mammalian gene circuit reveals antituberculosis compounds, *Proc Natl Acad Sci U S A*, 105 (2008) 9994-9998.
- [20] N. Willand, B. Folléas, C. Boutillon, L. Verbraeken, J.-C. Gesquière, A. Tartar, B. Deprez, Efficient, two-step synthesis of N-substituted nortropinone derivatives, *Tetrahedron Lett.*, 48 (2007) 5007-5011.
- [21] A.P. Mityuk, A.V. Denisenko, O.P. Dacenko, O.O. Grygorenko, P.K. Mykhailiuk, D.M. Volochnyuk, O.V. Shishkin, A.A. Tolmachev, An Approach to Azabicyclo[n.3.1]alkanes by Double Mannich Reaction, *Synthesis*, 2010 (2010) 493-497.
- [22] M.A. Brimble, C. Brocke, Efficient Synthesis of the Azabicyclo[3.3.1]nonane Ring System in the Alkaloid Methyllycaconitine Using Bis(alkoxymethyl)alkylamines as Aminoalkylating Agents in a Double Mannich Reaction, *Eur. J. Org. Chem.*, 2005 (2005) 2385-2396.
- [23] A.F. Abdel-Magid, S.J. Mehrman, A Review on the Use of Sodium Triacetoxyborohydride in the Reductive Amination of Ketones and Aldehydes, *Org. Process Res. Dev.*, 10 (2006) 971-1031.
- [24] Y. Zhao, W. Huang, L. Zhu, J. Hu, Difluoromethyl 2-pyridyl sulfone: a new gem-difluoroolefination reagent for aldehydes and ketones, *Org. Lett.*, 12 (2010) 1444-1447.
- [25] S.J. McGinty, A. Finch, R. Griffith, R.M. Graham, J.B. Bremner, Synthesis and biological evaluation of bicyclic and tricyclic substituted nortropine derivatives: discovery of a novel selective alpha1D-adrenergic receptor ligand, *Bioorg. Med. Chem.*, 12 (2004) 5639-5650.
- [26] N.A. Meanwell, Synopsis of some recent tactical application of bioisosteres in drug design, *J. Med. Chem.*, 54 (2011) 2529-2591.
- [27] W. Kabsch, XDS, *Acta Crystallogr D Biol Crystallogr*, 66 (2010) 125-132.
- [28] A. Vagin, A. Teplyakov, MOLREP: an Automated Program for Molecular Replacement, *J. Appl. Cryst.*, 30 (1997) 1022-1025.
- [29] G.N. Murshudov, P. Skubák, A.A. Lebedev, N.S. Pannu, R.A. Steiner, R.A. Nicholls, M.D. Winn, F. Long, A.A. Vagin, REFMAC5 for the refinement of macromolecular crystal structures, *Acta Crystallogr D Biol Crystallogr*, 67 (2011) 355-367.
- [30] P. Emsley, K. Cowtan, Coot: model-building tools for molecular graphics, *Acta Crystallogr D Biol Crystallogr*, 60 (2004) 2126-2132.
- [31] F. Long, R.A. Nicholls, P. Emsley, S. Gražulis, A. Merkys, A. Vaitkus, G.N. Murshudov, AceDRG: a stereochemical description generator for ligands, *Acta Crystallogr D Struct Biol*, 73 (2017) 112-122.
- [32] I.J. Tickle, Statistical quality indicators for electron-density maps, *Acta Crystallogr D Biol Crystallogr*, 68 (2012) 454-467.
- [33] V.B. Chen, W.B. Arendall, J.J. Headd, D.A. Keedy, R.M. Immormino, G.J. Kapral, L.W. Murray, J.S. Richardson, D.C. Richardson, MolProbity: all-atom structure validation for macromolecular crystallography, *Acta Crystallogr D Biol Crystallogr*, 66 (2010) 12-21.